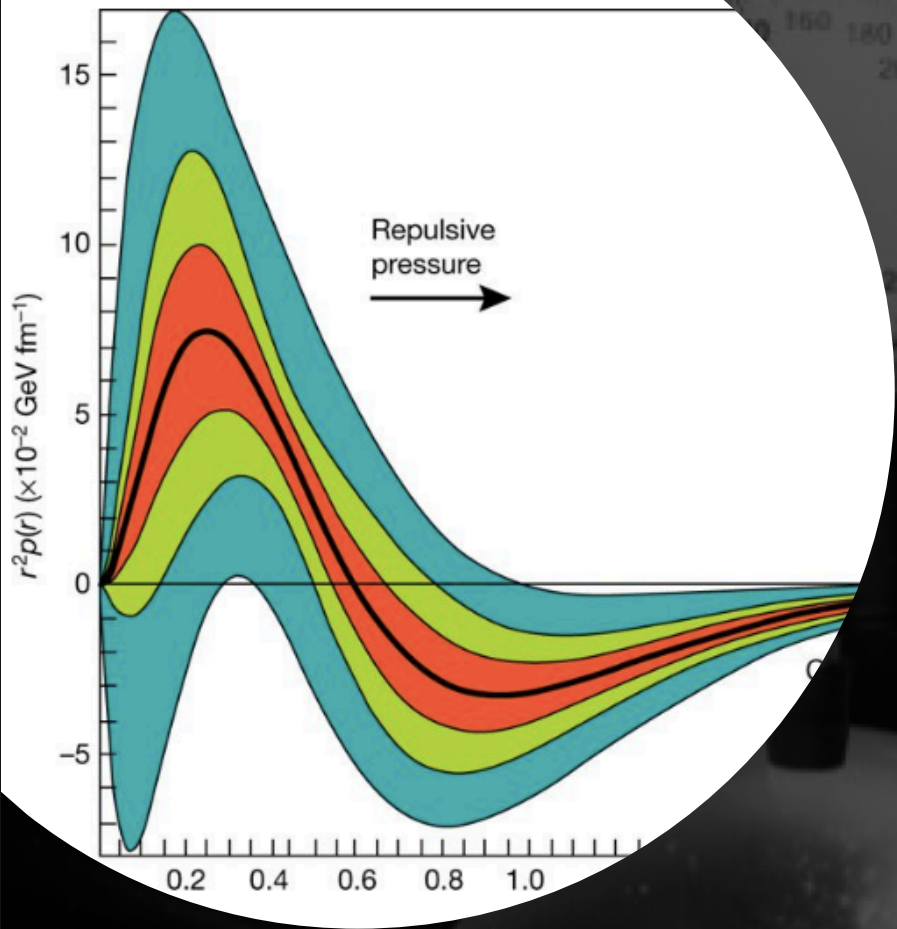


Nuclear femtography as a
bridge from the nucleon to
neutron stars

Strong QCD
Jefferson Lab
November 6-8, 2019

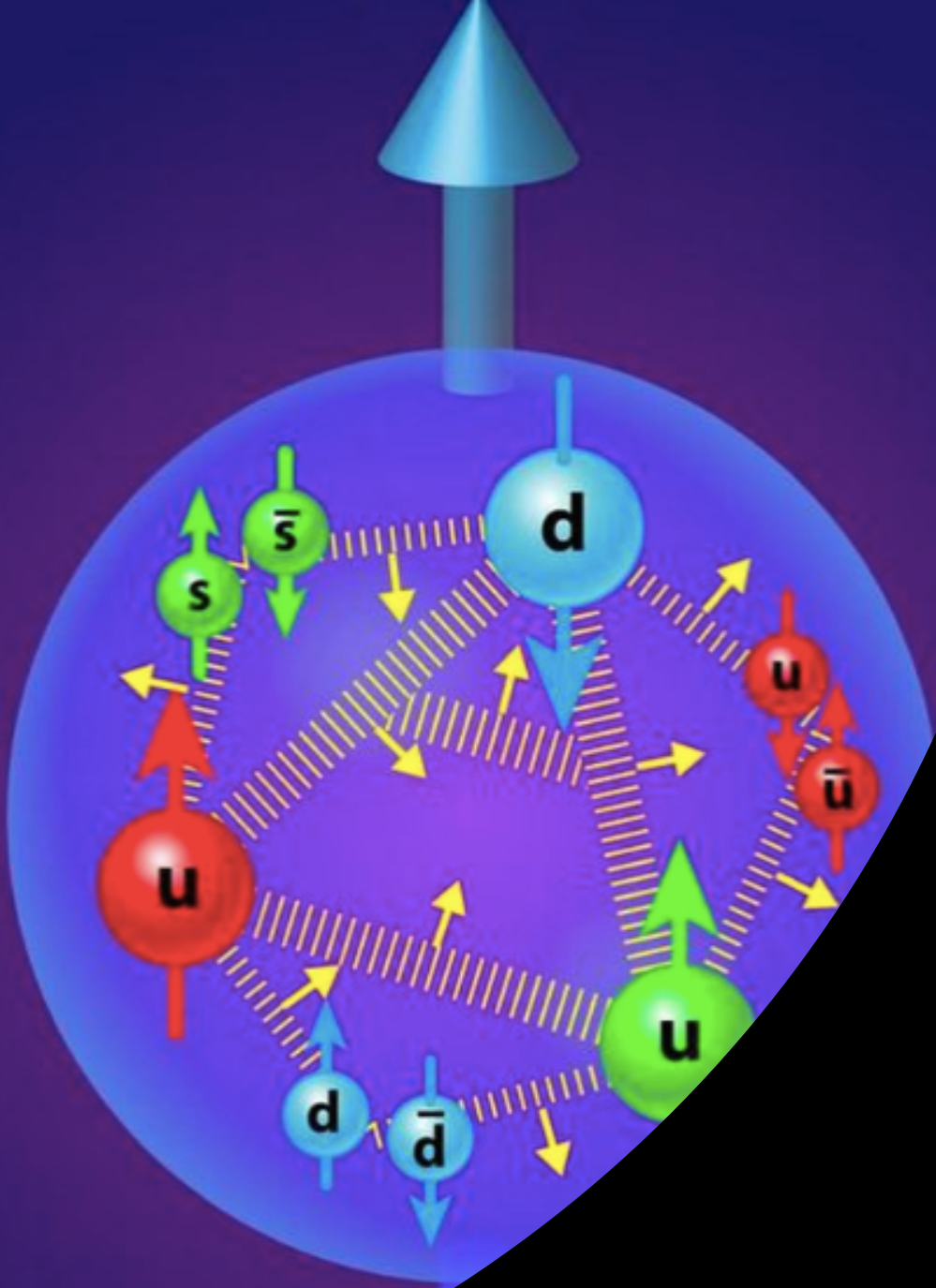
SIMONETTA LIUTI

UNIVERSITY OF VIRGINIA



Burkert, Elouadrhiri, Girod,
Nature 557, 396 (2018)

- “The average peak pressure near the center is about 10^{35} pascals, which exceeds the pressure estimated for the most densely packed known objects in the Universe, neutron stars”



How is the pressure distribution extracted from data?

(How does the proton/neutron get its mass and spin?)

Evaluating the mechanical properties of the proton

$$\mathcal{L}_{QCD} = \bar{\psi} (i\gamma_{\mu} D^{\mu} - m) \psi - \frac{1}{4} F_{a,\mu\nu} F_a^{\mu\nu}$$

Invariance of \mathcal{L}_{QCD} under **translations** and **rotations**

Energy Momentum Tensor

from **translation** inv.



$$T_{QCD}^{\mu\nu} = \frac{1}{4} \bar{\psi} \gamma^{(\mu} D^{\nu)} \psi + Tr \left\{ F^{\mu\alpha} F_{\alpha}^{\nu} - \frac{1}{2} g^{\mu\nu} F^2 \right\}$$

Angular Momentum Tensor

from **rotation** inv.



$$M_{QCD}^{\mu\nu\lambda} = x^{\nu} T_{QCD}^{\mu\lambda} - x^{\lambda} T_{QCD}^{\mu\nu}$$

The QCD Energy Momentum Tensor

Mass		$\frac{E^2 + B^2}{2}$	S_x	S_y	S_z
	Momentum density	S_x	σ_{xx}	σ_{xy}	σ_{xz}
		S_y	σ_{yx}	σ_{yy}	σ_{yz}
		S_z	σ_{zx}	σ_{zy}	σ_{zz}

Momentum density

Shear stress

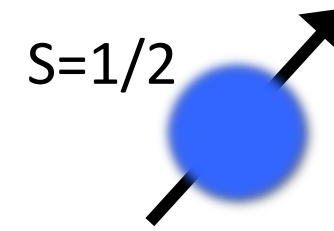
Pressure

$$T^{\mu\nu} = \frac{1}{4} i q \bar{\psi} (\gamma^\mu \vec{D}^\nu + \gamma^\nu \vec{D}^\mu) \psi + Tr \left\{ F^{\mu\alpha} F_\alpha^\nu - \frac{1}{2} g^{\mu\nu} F^2 \right\}$$



$$M^{\mu\nu\lambda} = x^\nu T^{\mu\lambda} - x^\lambda T^{\mu\nu}$$

Angular Momentum density



QCD EMT matrix element between proton states (X. Ji, 1997)

$$\begin{aligned}
 \langle p', \Lambda | T_{\mathbf{q}, \mathbf{g}}^{\mu\nu} | p, \Lambda \rangle = & A(t) \bar{U}(p', \Lambda') [\gamma^\mu P^\nu + \gamma^\nu P^\mu] U(p, \Lambda) + B(t) \bar{U}(p', \Lambda') i \frac{\sigma^{\mu(\nu} \Delta^{\nu)} }{2M} U(p, \Lambda) \\
 & + C(t) [\Delta^2 g^{\mu\nu} - \Delta^{\mu\nu}] \bar{U}(p', \Lambda') U(p, \Lambda) + \tilde{C}(t) g^{\mu\nu} \bar{U}(p', \Lambda') U(p, \Lambda)
 \end{aligned}$$

forward

off-forward

q and g not separately conserved

$$\left\{ \begin{aligned}
 P &= \frac{p + p'}{2} \\
 \Delta &= p' - p = q - q' \\
 t &= (p - p')^2 = \Delta^2
 \end{aligned} \right.$$

Direct calculation of EMT form factors

Donoghue et al. PLB529 (2002),

A. Freese , QCD Evolution 2019

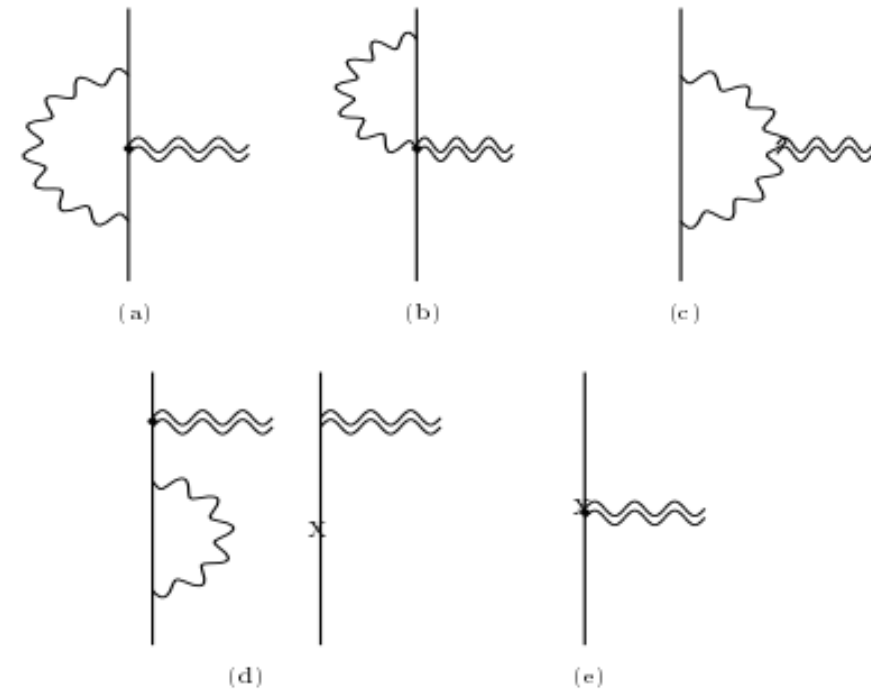
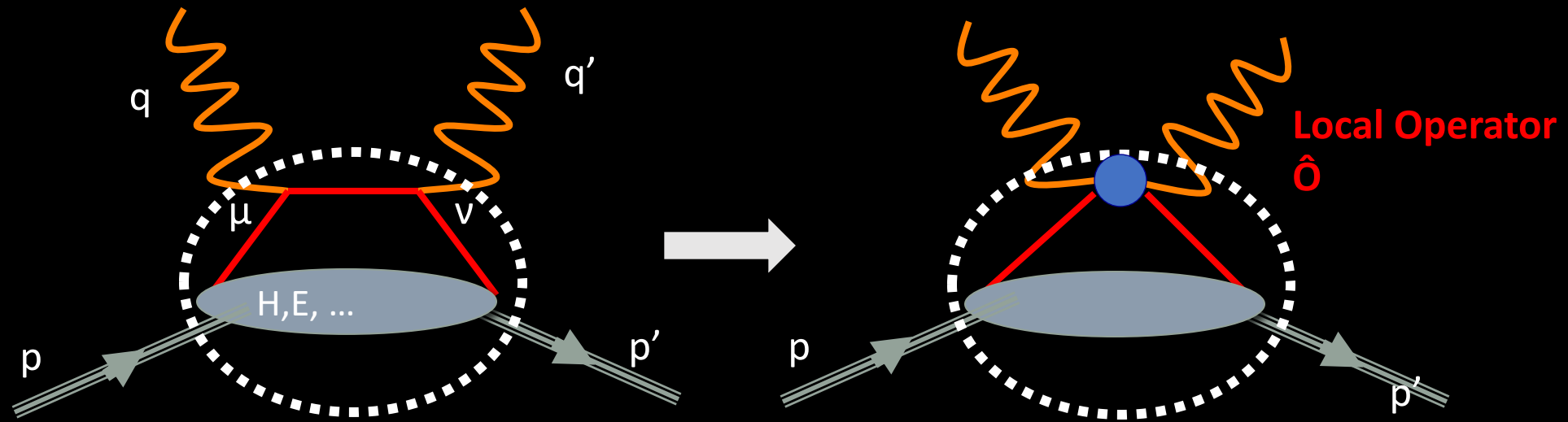


Figure 2: Feynman diagrams for spin 1/2 radiative corrections to $T_{\mu\nu}$.

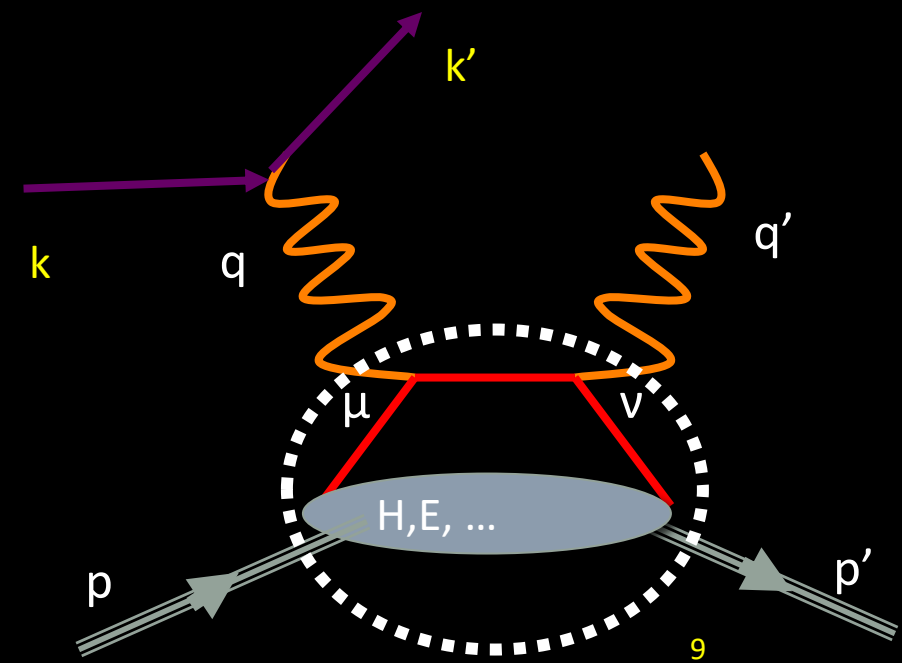
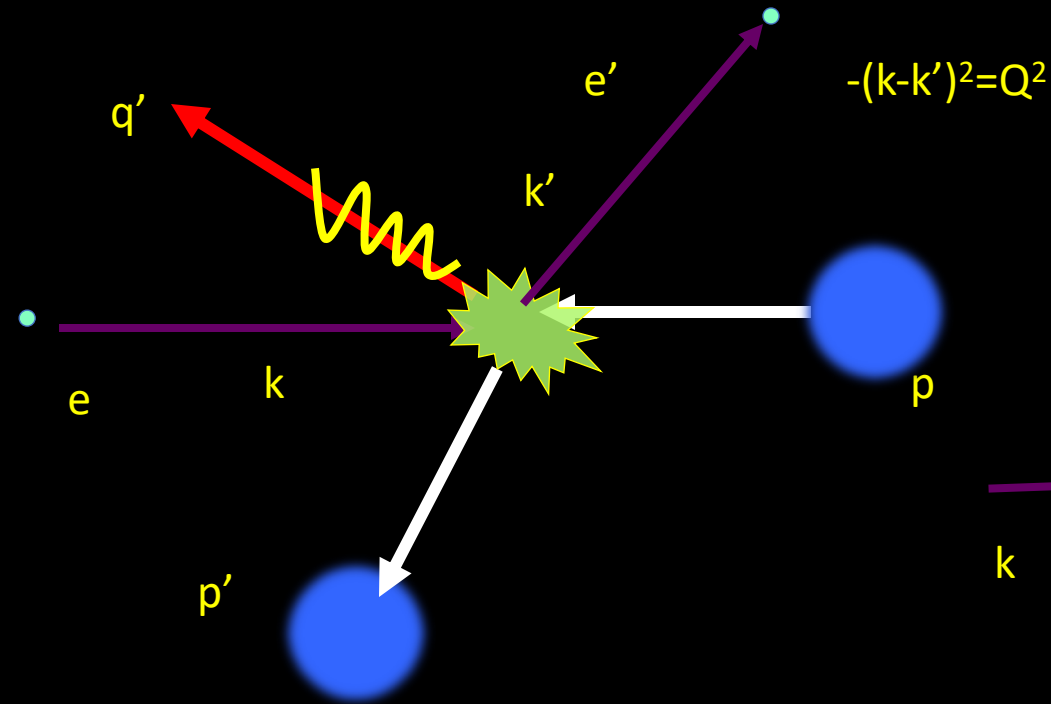
EMT matrix elements from Generalized Parton Distributions Moments



- Large momentum transfer $Q^2 \gg M^2 \Rightarrow$ “deep”
- Large Invariant Mass $W^2 \gg M^2 \Rightarrow$ equivalent to an “inelastic” process

Deeply Virtual Compton Scattering

$$ep \rightarrow e' \gamma' p'$$



2nd Mellin moments

From OPE ↔ From EMT

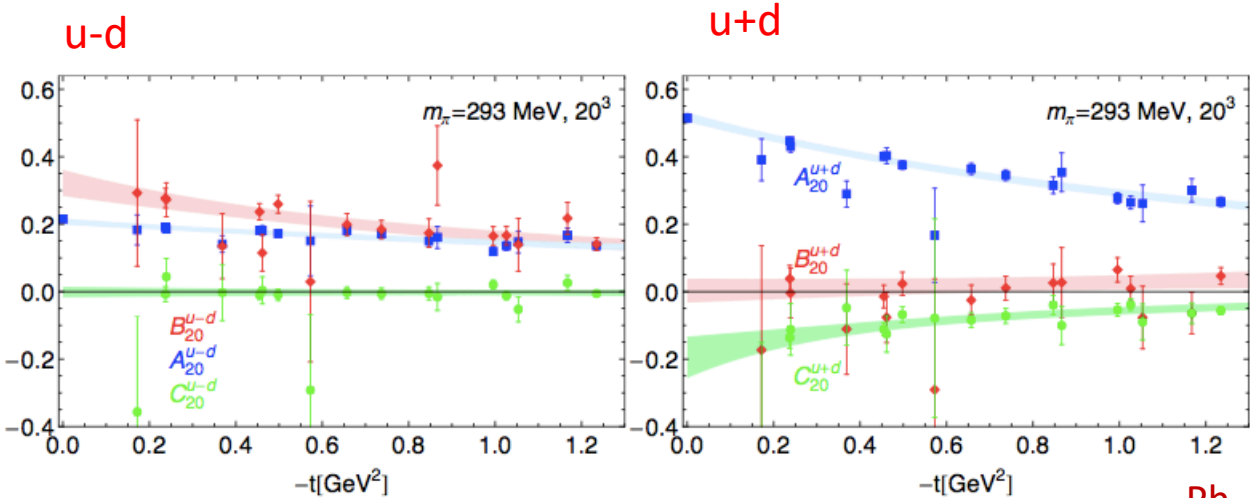
$$\int dx x H(x, \xi, t) = A_{20}(t) + \xi^2 C_{20}(t) \equiv A(t) + \xi^2 C(t) \leftarrow \text{D-term}$$
$$\int dx x E(x, \xi, t) = B_{20}(t) - \xi^2 C_{20}(t) \equiv B(t) - \xi^2 C(t)$$

Physical interpretation of EMT form factors

$$\frac{1}{2} (A_q + B_q) = \boxed{J_q} = \frac{1}{2} (A_{20} + B_{20}) \rightarrow J_q^i = \int d^3r \epsilon^{ijk} r_j T_{0k}$$

$$A_q = \boxed{\langle x_q \rangle} = A_{20}$$

$$C_q = \boxed{\text{Internal Forces}} = C_{20} \rightarrow \int d^3r (r^i r^j - \delta^{ij} r^2) T_{ij}$$



C (D-term) is related to pressure

Static approximation

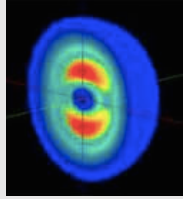
$$T_{ij} = \left(\frac{r_i r_j}{r^2} - \frac{1}{3} \delta_{ij} \right) s(r) + \delta_{ij} p(r)$$

Landau&Lifshitz, Vol.7

M. Polyakov, hep-ph/0210165

M. Polyakov, P. Schweitzer, arXiv:1805.06596

C is a measure of the **Elastic Free Energy** in the proton

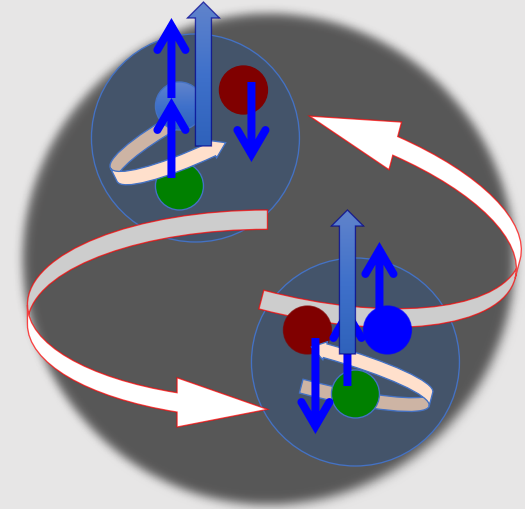


Angular momentum sum rule for spin one hadronic systems

Swadhin K. Taneja,^{1,*} Kunal Kathuria,^{2,†} Simonetta Liuti,^{2,‡} and Gary R. C. S. Klein^{3,§}

PRD86(2012)

7 conserved form factors!



$$\begin{aligned}
 \langle p', \Lambda' | T^{\mu\nu} | p, \Lambda \rangle = & -\frac{1}{2} P^\mu P^\nu (\epsilon'^* \epsilon) \mathcal{G}_1(t) - \frac{1}{4} P^\mu P^\nu \frac{(\epsilon P)(\epsilon'^* P)}{M^2} \mathcal{G}_2(t) \\
 & -\frac{1}{2} [\Delta^\mu \Delta^\nu - g^{\mu\nu} \Delta^2] (\epsilon'^* \epsilon) \mathcal{G}_3(t) - \frac{1}{4} [\Delta^\mu \Delta^\nu - g^{\mu\nu} \Delta^2] \frac{(\epsilon P)(\epsilon'^* P)}{M^2} \mathcal{G}_4(t) \\
 & + \frac{1}{4} [(\epsilon'^*{}^\mu (\epsilon P) + \epsilon^\mu (\epsilon'^* P)) P^\nu + \mu \leftrightarrow \nu] \mathcal{G}_5(t) \\
 & + \frac{1}{4} [(\epsilon'^*{}^\mu (\epsilon P) - \epsilon^\mu (\epsilon'^* P)) \Delta^\nu + \mu \leftrightarrow \nu + 2g_{\mu\nu} (\epsilon P)(\epsilon'^* P) - (\epsilon'^*{}^\mu \epsilon^\nu + \epsilon'^*{}^\nu \epsilon^\mu) \Delta^2] \mathcal{G}_6(t) \\
 & + \frac{1}{2} [\epsilon'^*{}^\mu \epsilon^\nu + \epsilon'^*{}^\nu \epsilon^\mu] \mathcal{G}_7(t) + g^{\mu\nu} (\epsilon'^* \epsilon) M^2 \mathcal{G}_8(t)
 \end{aligned}$$

General rule to count form factors: t-channel J^{PC} q. numbers

n	$J^{PC}(S; L)$				
0	0^{+-}	$1^{--}(1; 0, 2)$			
1	$0^{++}(1; 1)$	1^{-+}	$2^{++}(1; 1, 3)$		
2	0^{+-}	$1^{--}(1; 0, 2)$	2^{+-}	$3^{--}(1; 2, 4)$	
3	$0^{++}(1; 1)$	1^{-+}	$2^{++}(1; 1, 3)$	3^{-+}	$4^{++}(1; 3, 5)$
...			...		

Haegler, PLB(2004)
Z.Chen&Ji, PRD(2005)

TABLE III: J^{PC} of the vector operators with $(S; L, L')$ for the corresponding $N\bar{N}$ state. Where there are no $(S; L, L')$ values there are no matching quantum numbers for the $N\bar{N}$ system.

Nucleon

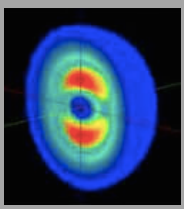
	$L = 0$	1	2	3	4	...
$S = 0$	$J^{PC} 0^{-+}$	1^{+-}	2^{-+}	3^{+-}	4^{-+}	
$S = 1$	1^{--}	0^{++}	1^{--}	2^{++}	3^{--}	
		1^{++}	2^{--}	3^{++}	4^{--}	
		2^{++}	3^{--}	4^{++}	5^{--}	

TABLE I: J^{PC} of the $N\bar{N}$ states.

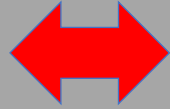
Deuteron

	$L = 0$	1	2	3	4	...
$S = 0$	$J^{PC} 0^{++}$	1^{--}	2^{++}	3^{--}	4^{++}	
$S = 1$	1^{+-}	0^{-+}	1^{+-}	2^{-+}	3^{+-}	
		1^{-+}	2^{+-}	3^{-+}	4^{+-}	
		2^{-+}	3^{+-}	4^{-+}	5^{+-}	
$S = 2$	2^{++}	1^{--}	0^{++}	1^{--}	2^{++}	
		2^{--}	1^{++}	2^{--}	3^{++}	
		3^{--}	2^{++}	3^{--}	4^{++}	
			3^{++}	4^{--}	5^{++}	
			4^{++}	5^{--}	6^{++}	

TABLE II: J^{PC} of the $d\bar{d}$ states.



From OPE



From EMT

$$2 \int dxx [H_1(x, \xi, t) - \frac{1}{3} H_5(x, \xi, t)] = \mathcal{G}_1(t) + \xi^2 \mathcal{G}_3(t)$$

Momentum

$$2 \int dxx H_2(x, \xi, t) = \mathcal{G}_5(t)$$

Angular Momentum

Double flip

D-term dependent
on polarization

$$2 \int dxx H_3(x, \xi, t) = \mathcal{G}_2(t) + \xi^2 \mathcal{G}_4(t)$$

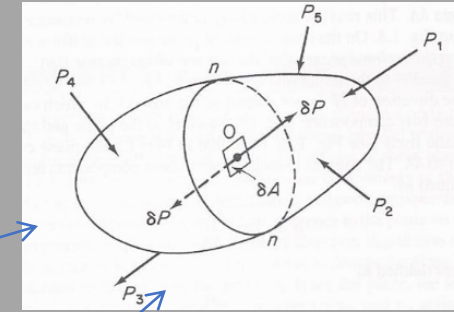
Quadrupole

$$-4 \int dxx H_4(x, \xi, t) = \xi \mathcal{G}_6(t)$$

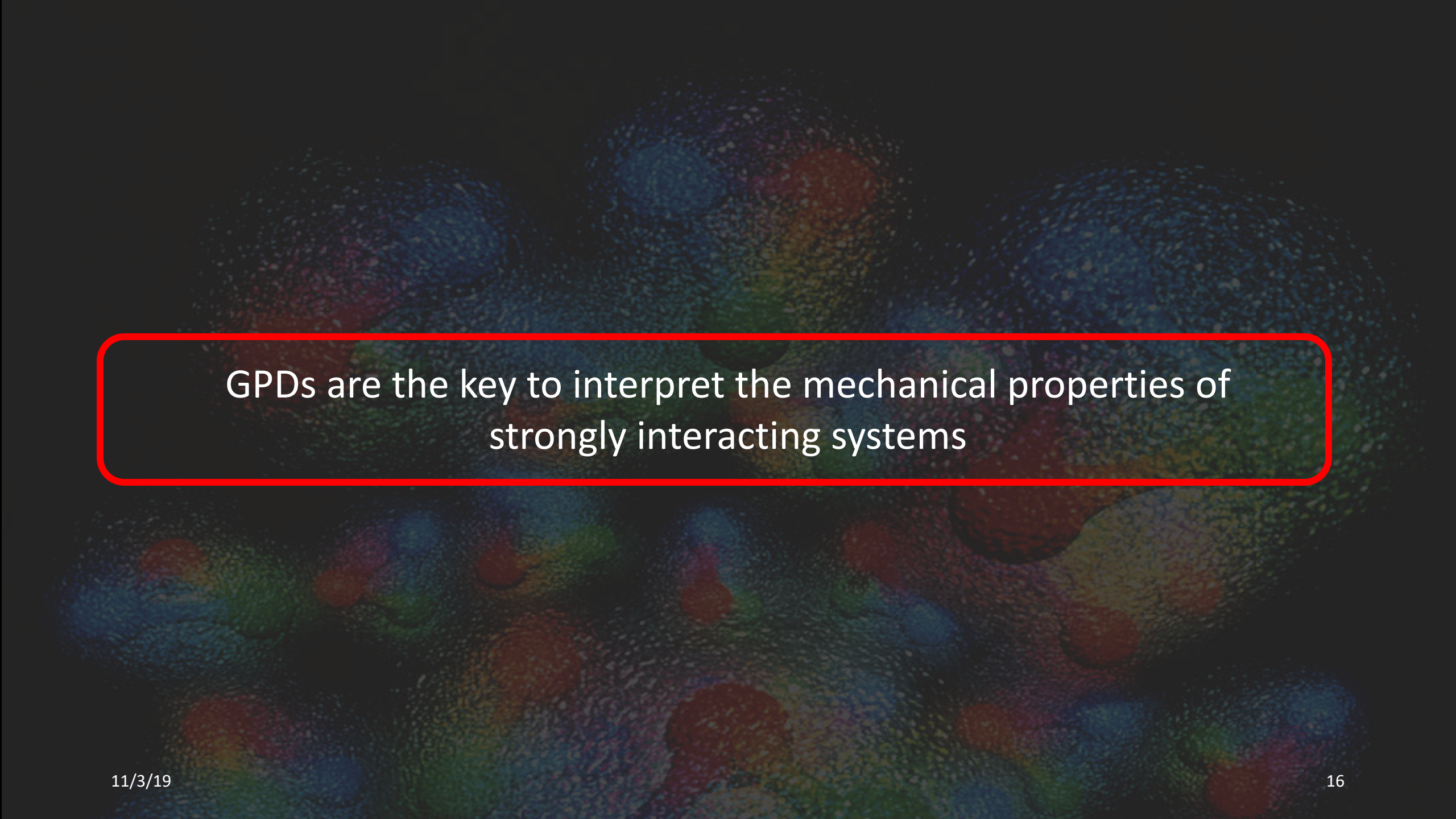
ξ -odd

$$\int dxx H_5(x, \xi, t) = -\frac{t}{8M_D^2} \mathcal{G}_6(t) + \frac{1}{2} \mathcal{G}_7(t)$$

Connected to b_1 SR

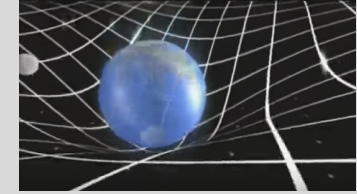


Connecting with observables: work in progress with Brandon Kriesten, Abha Rajan Swadhin Taneja



GPDs are the key to interpret the mechanical properties of
strongly interacting systems

EMT: source of the gravitational field



action

$$S = \int \sqrt{-g} \left[\frac{1}{16\pi G} \mathcal{R} - \mathcal{L}_m \right] d^4x$$

Ricci scalar \rightarrow curvature Flat space

Matter and energy in the universe \rightarrow $T_{\mu\nu} = \frac{\delta \mathcal{L}_m}{\delta g^{\mu\nu}} + g_{\mu\nu} \mathcal{L}_m$

Space-time geometry \rightarrow $G_{\mu\nu} = R_{\mu\nu} - \frac{1}{2} g_{\mu\nu} R$
Ricci tensor

Einstein's Eqs. \rightarrow $G_{\mu\nu} = 8\pi G T_{\mu\nu}$

Using the metric, $g_{\mu\nu}$, one can calculate:

- the curvature tensor $R_{\mu\nu}$
- the Einstein tensor $G_{\mu\nu}$
- the stress energy tensor for a perfect fluid:

$$T_{\mu\nu} = (p + \epsilon)u_{\mu}u_{\nu} + pg_{\mu\nu}$$

TOV Equations

$$\frac{dp(r)}{dr} = -\frac{G}{r} (\epsilon(r) + p(r)) (m(r) + 4\pi r^3 p(r)) (r - 2Gm(r))^{-1}$$

$$\frac{dm(r)}{dr} = 4\pi r^2 \epsilon(r)$$

EoS $p(r)$ - $\epsilon(r)$ relation

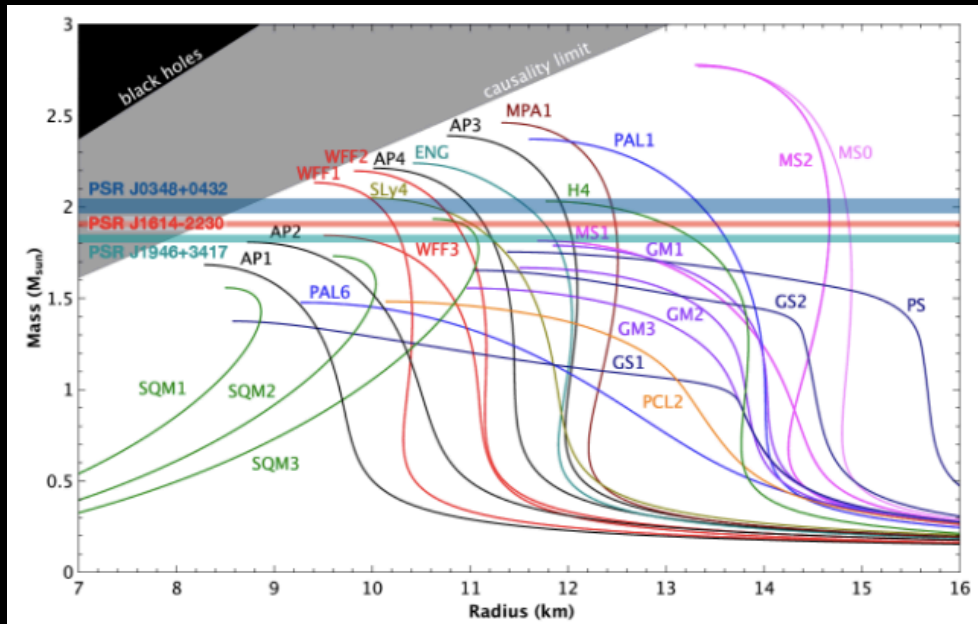
energy density

pressure

matter distribution

Knowing the EoS one can solve TOV to find the mass-radius relation

Constraints from Pulsar Masses

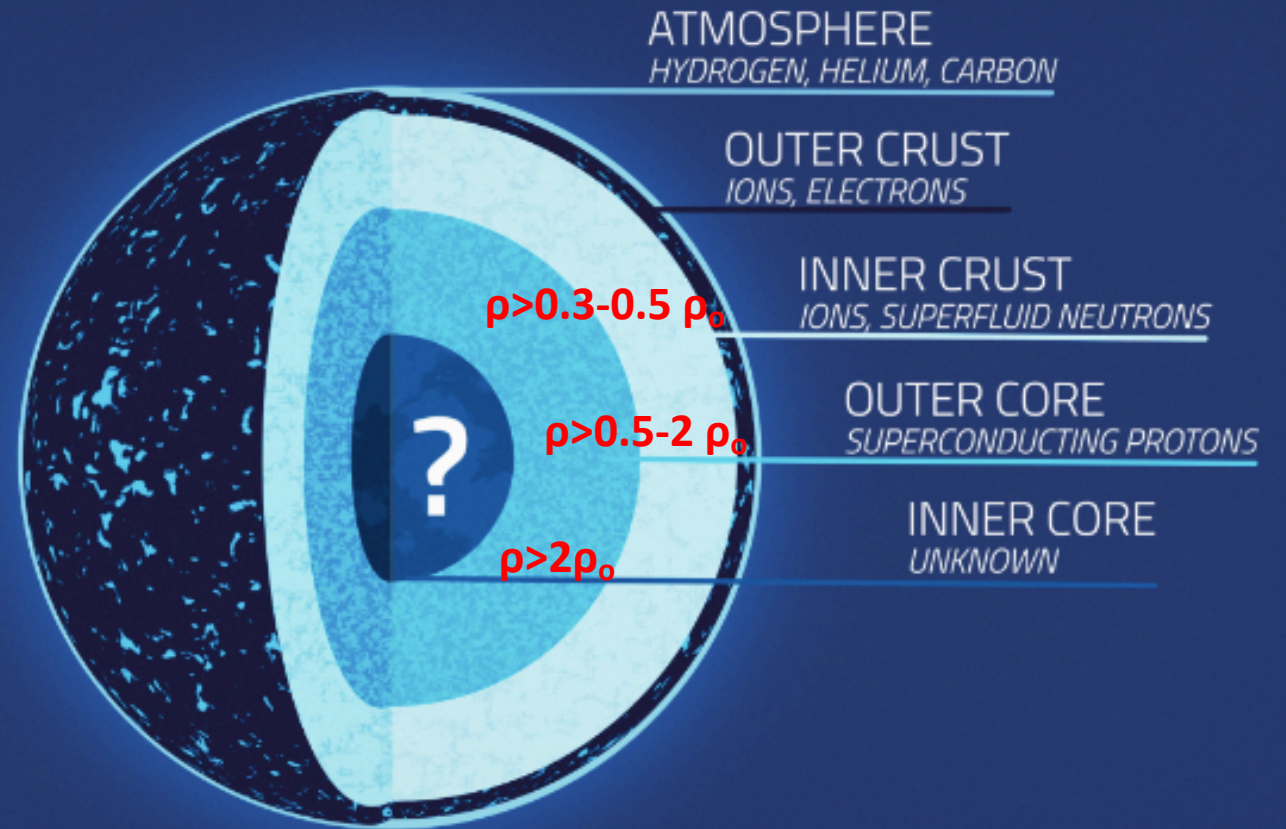


Özel and Freire, <http://xtreme.as.arizona.edu/NeutronStars>

J. Antoniadis et al., *Science* 340, 6131 (2013)
P. B. Demorest et al., *Nature* 467 (2010)

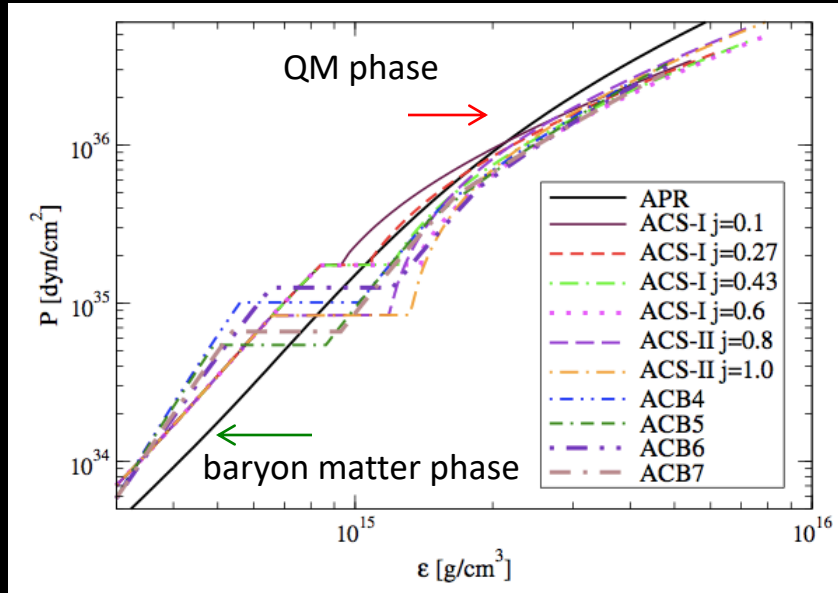
Constraints require the EoS to be stiff → consistent with predictions for ordinary nuclear matter composed of mostly neutrons and few protons including three body interactions

What governs
the EoS of
neutron stars?

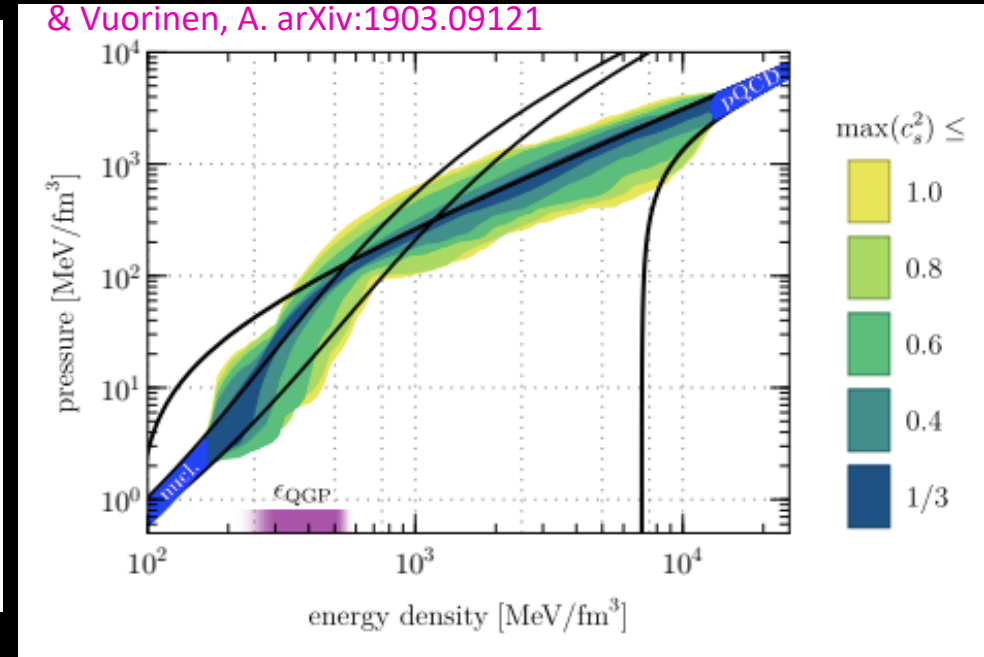


<https://svs.gsfc.nasa.gov/20267>

Pascalidhis et al., arXiv:1712.00451



Annala, E., Gorda, T., Kurkela, A., Nattila, J., & Vuorinen, A. arXiv:1903.09121



“...the existence of quark-matter cores inside very massive NSs should be considered the standard scenario, not an exotic alternative. QM is altogether absent in NS cores only under very specific conditions...”

- We propose a new, model independent way of evaluating the EoS in the quark matter phase by inferring it directly from the matrix elements of the QCD Energy Momentum Tensor (EMT) between nucleon states → **GPDs**
- **Model independent means relating measurement to measurement**
- This allows us to introduce **spatial coordinates/distance** in a novel way

Based on

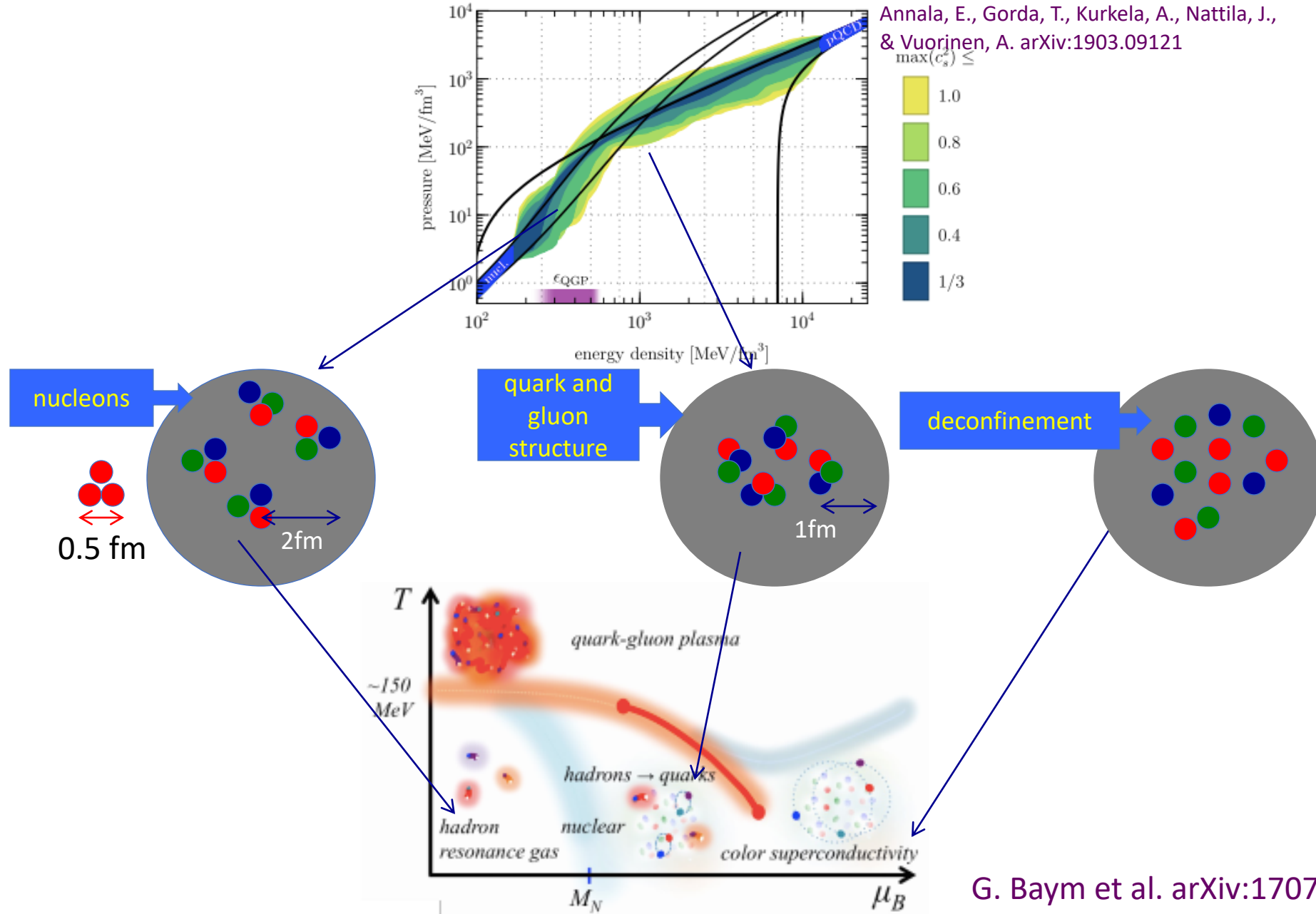
Bounds on the Equation of State of Neutron Stars from High Energy Deeply Virtual Exclusive Experiments

Abha Rajan,^{1,*} Tyler Gorda,^{2,†} Simonetta Liuti,^{2,‡} and Kent Yagi^{2,§}
¹Physics Department, Brookhaven National Laboratory, Upton, New York 11973, USA.
²Department of Physics, University of Virginia, Charlottesville, VA 22904, USA.

The recent detection of gravitational waves from merging neutron star events has opened a new window on the many unknown aspects of their internal dynamics. A key role in this context is played by the transition from baryon to quark matter described in the neutron star equation of state (EoS). In particular, the binary pulsar observation of heavy neutron stars requires appropriately stiff dense matter in order to counter gravitational collapse, at variance with the predictions of many phenomenological quark models. On the other side, the LIGO observations favor a softer EoS therefore providing a lower bound to the equation stiffness. We introduce a quantum chromodynamics (QCD) description of the neutron star's high baryon density regime where the pressure and energy density distributions are directly obtained from the matrix elements of the QCD energy momentum tensor. Recent ab initio calculations allow us to evaluate the energy-momentum tensor in a model independent way including both quark and gluon degrees of freedom. Our approach is a first effort to replace quark models and effective parton distributions with a first principles, fully QCD-based description. Most importantly, the QCD energy momentum tensor matrix elements are connected to the Mellin moments of the generalized parton distributions which can be measured in deeply virtual exclusive scattering experiments. As a consequence, we establish a connection between observables from high energy experiments and from the analysis of gravitational wave events. Both can be used to mutually constrain the respective sets of data. In particular, the emerging QCD-based picture is consistent with the GW170817 neutron star merger event once we allow a first-order phase transition low-density nuclear matter EoS to the newly-constructed high-density quark-gluon one.

arXiv:1812.01479

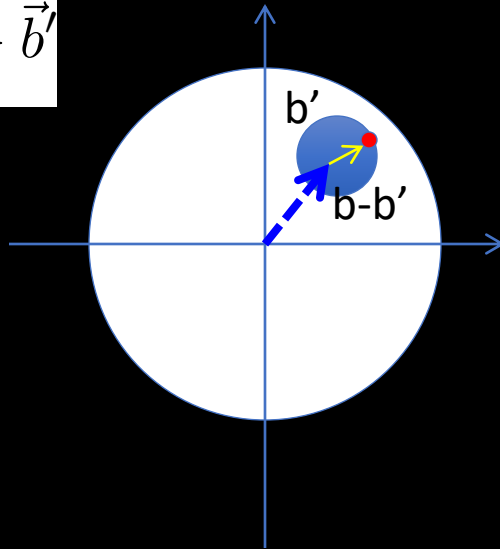
Densities and distance scales



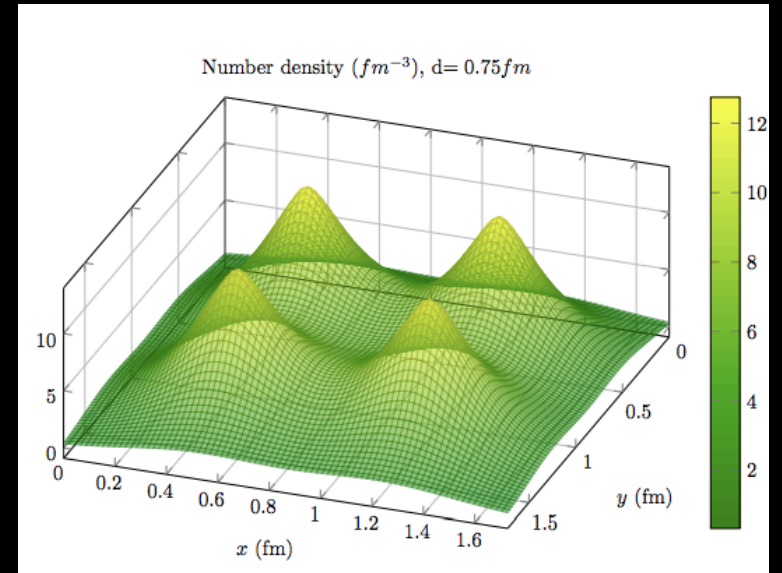
Nuclear Spatial Density

$$q_A(b) = \int d^2b' \rho_A(|\vec{b} - \vec{b}'|) q_N(b')$$

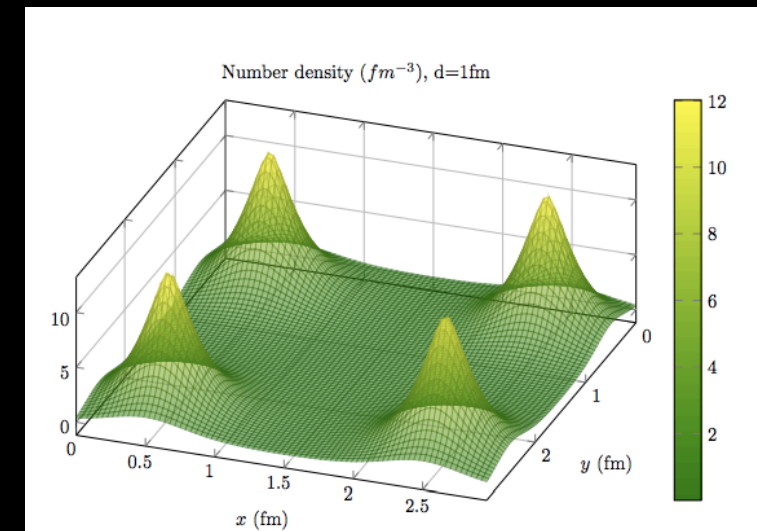
$$\approx k_F^3 \int d^2\beta q_N(|\vec{b} - \vec{\beta}|), \quad \vec{\beta} = \vec{b} - \vec{b}'$$



d = 0.75 fm

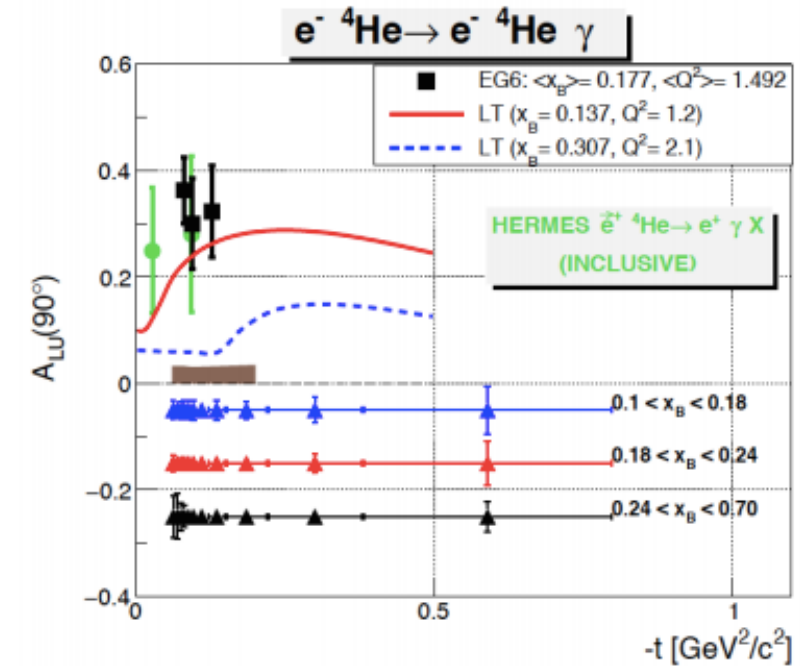
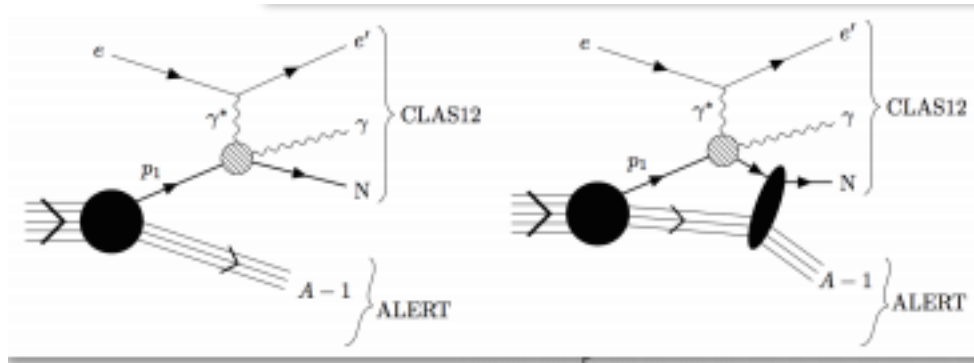


d = 2 fm



ALERT Proposal at Jefferson Lab: Nuclear Exclusive and Semi-inclusive Measurements with A New CLAS12 Low Energy Recoil Tracker

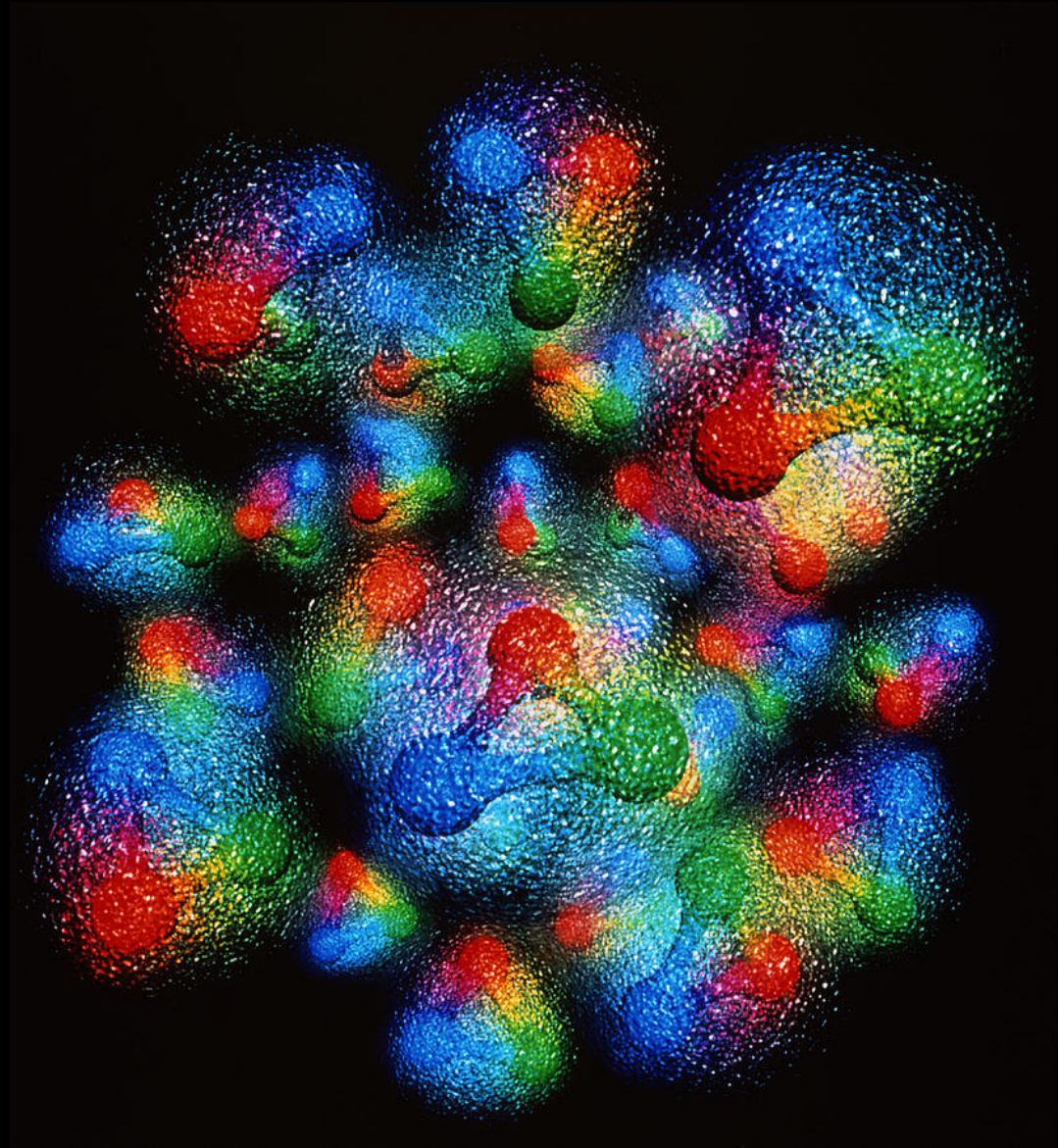
W. Armstrong. M. Hattawy, ...



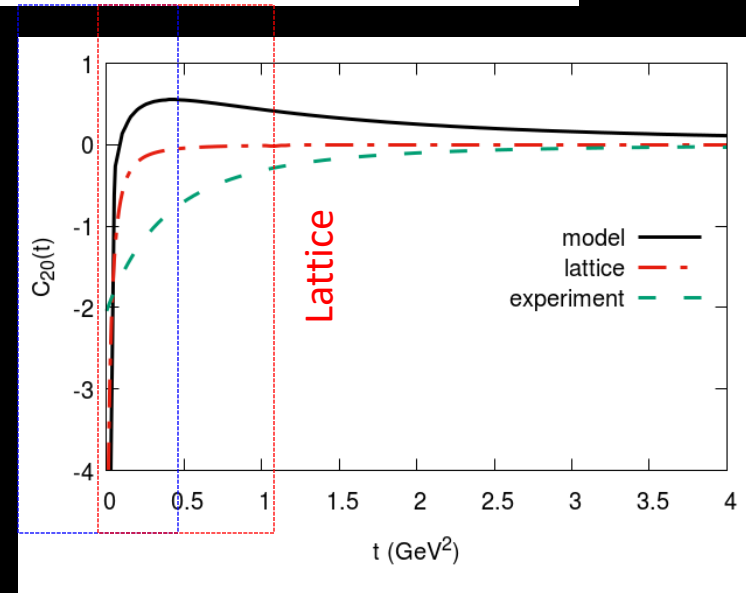
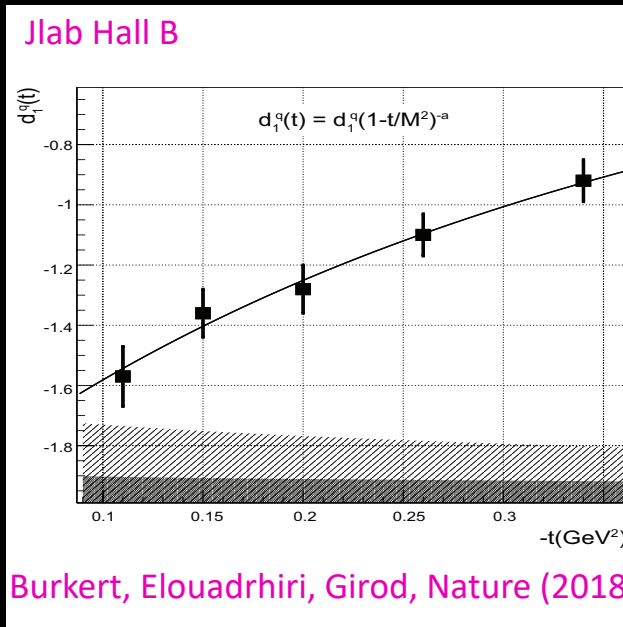
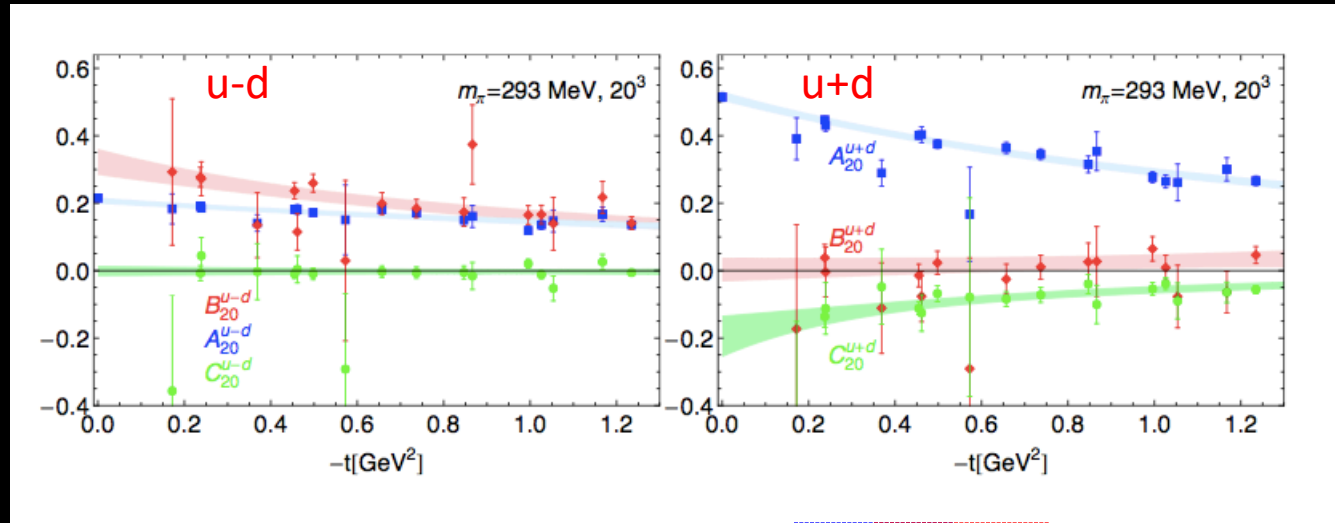
$S=0$

$$\langle p' | T^{\mu\nu} | p \rangle = 2 \left[A(t) P^\mu P^\nu + C(t) (\Delta^2 g^{\mu\nu} - \Delta^\mu \Delta^\nu) \right] + \tilde{C}(t) g^{\mu\nu}$$

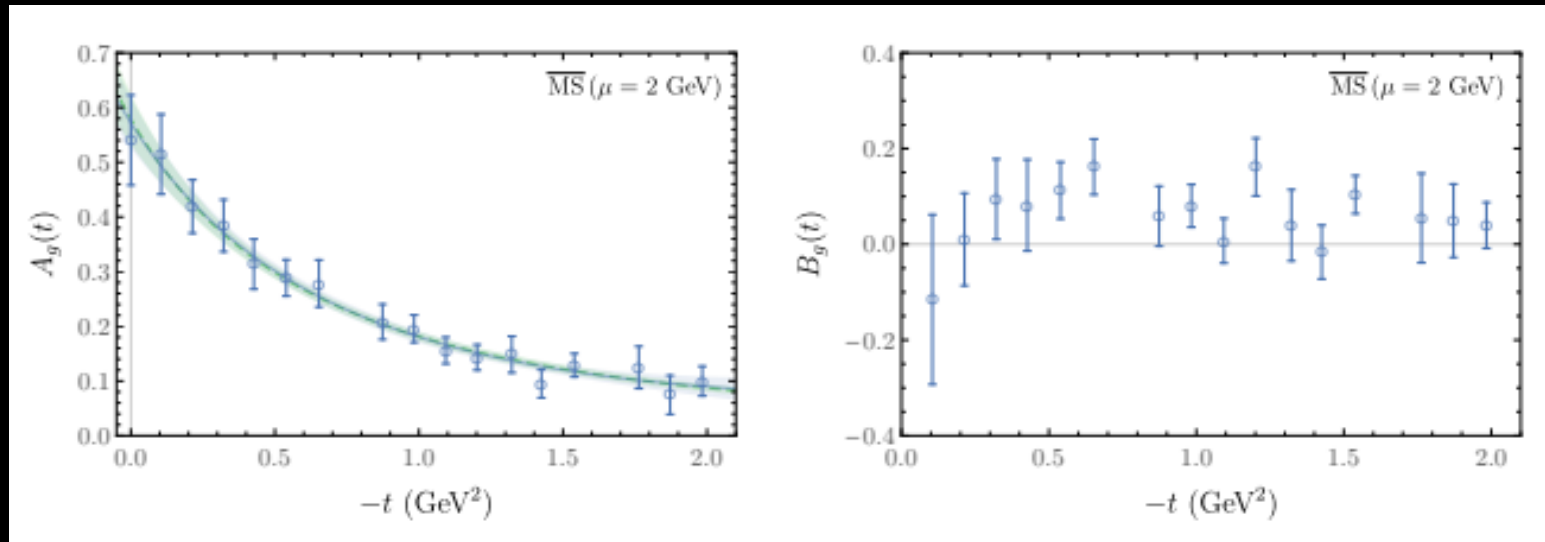
Nucleon
Gravitomagnetic
Form Factors



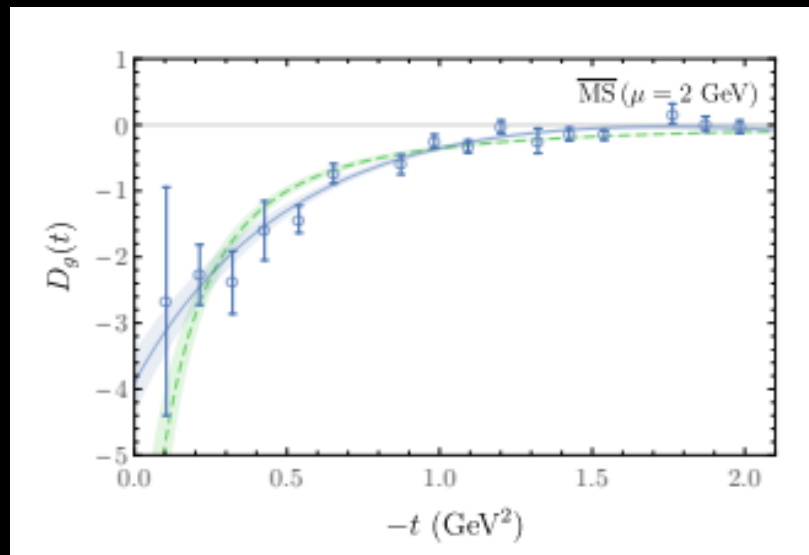
C₂₀



Gluons

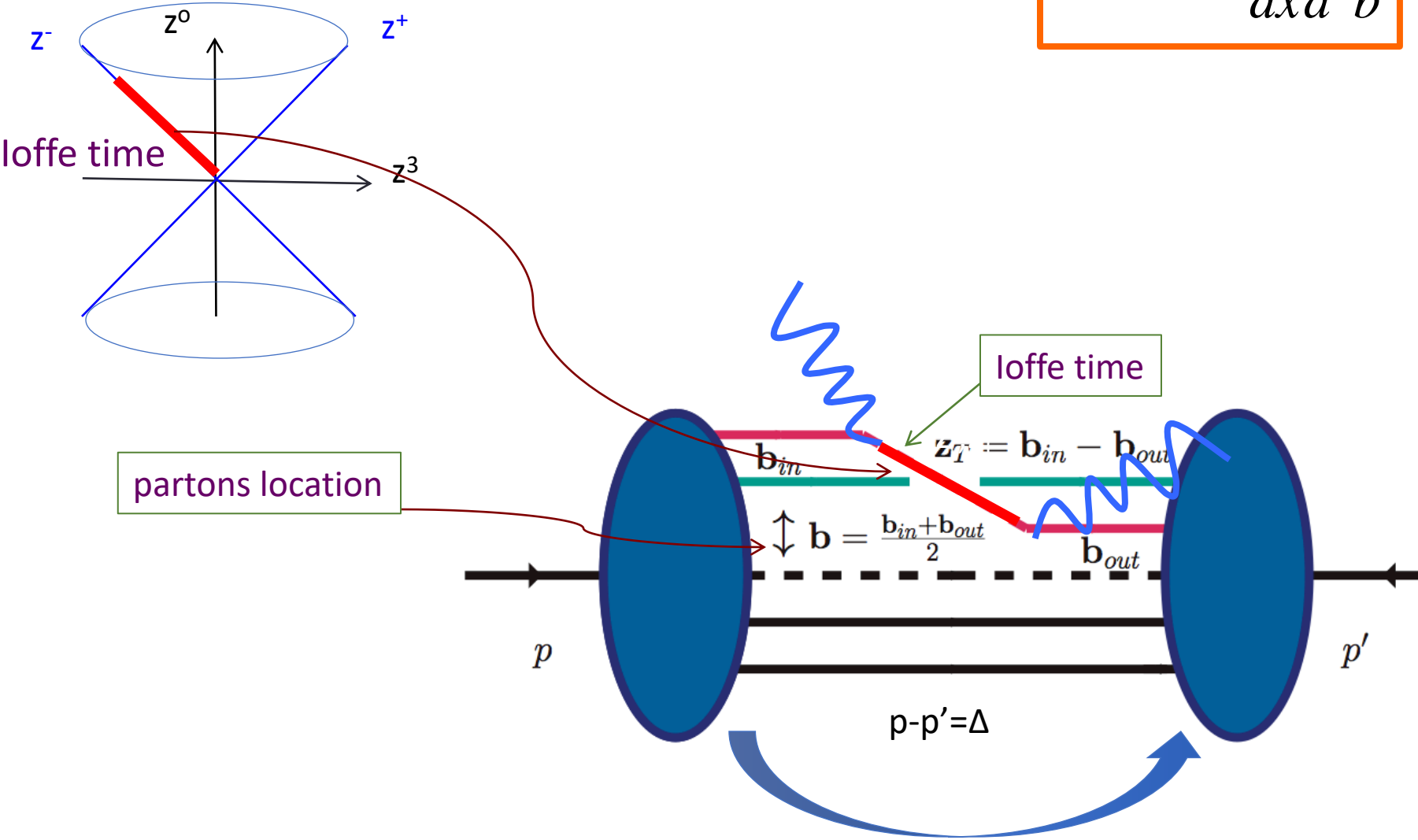


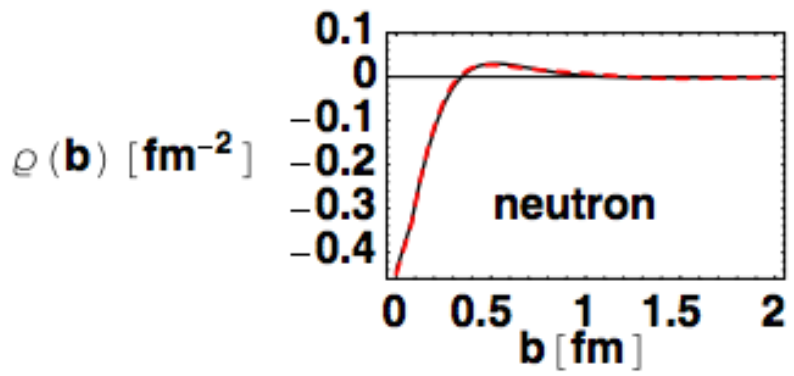
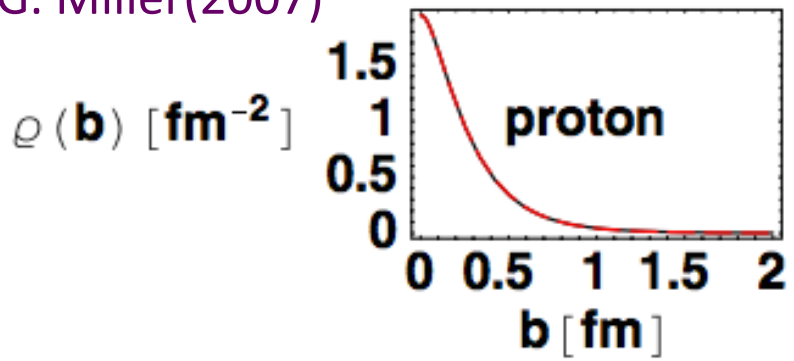
$m_\pi = 450 \text{ MeV}$



Two distinct distance scales

$$q(x, \vec{b}) = \frac{dn}{dx d^2 \vec{b}}$$





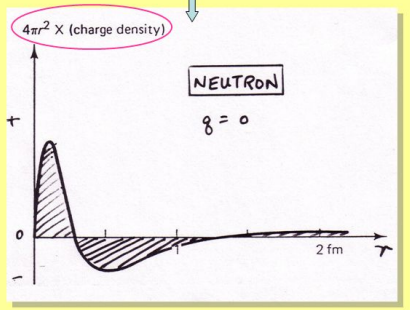
Using $q(x, \vec{b}) = \frac{dn}{dx d^2\vec{b}}$ we can map out faithfully the spatial quark distributions in the transverse plane (no modeling/approximation)

Neutron “textbook” density

What does negative $\langle r^2 \rangle$ mean? 4

$$\langle r^2 \rangle \equiv \int r^2 \rho(r) d^3r = \int r^2 (4\pi r^2 \rho(r)) dr$$

- charge density must have both -ve and +ve regions, since net charge = 0
- integral is weighted with $r^2 \rightarrow$ more negative charge at large radius



Including all polarization configurations:

$$\rho_{\Lambda\lambda}^q(\mathbf{b}) = H_q(\mathbf{b}^2) + \frac{b^i}{M} \epsilon_{ij} S_T^j \frac{\partial}{\partial b} E_q(\mathbf{b}^2) + \Lambda\lambda \tilde{H}_q(\mathbf{b}^2),$$

1st Mellin M.

$$H_q(\mathbf{b}^2) = \int \frac{d^2 \Delta_T}{(2\pi)^2} e^{i\Delta_T \cdot \mathbf{b}} A_1^q(t);$$

number/mass density

2nd Mellin M.

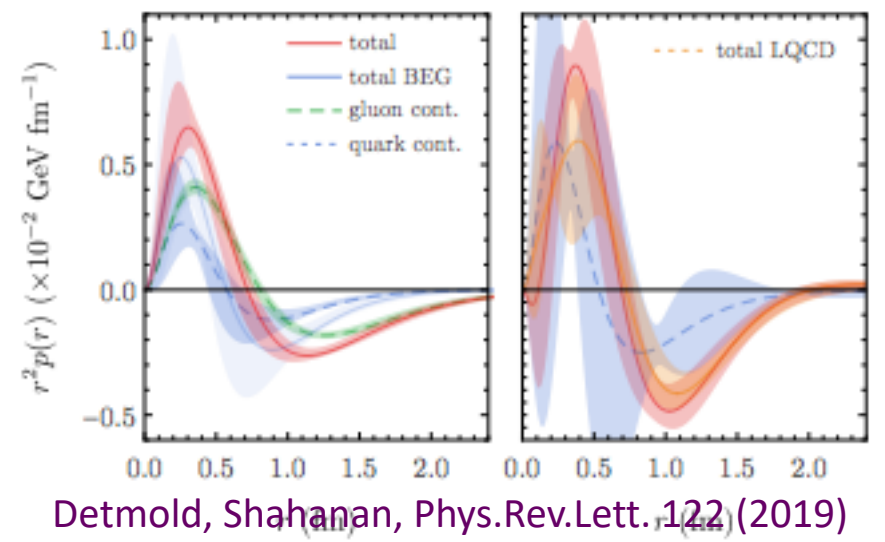
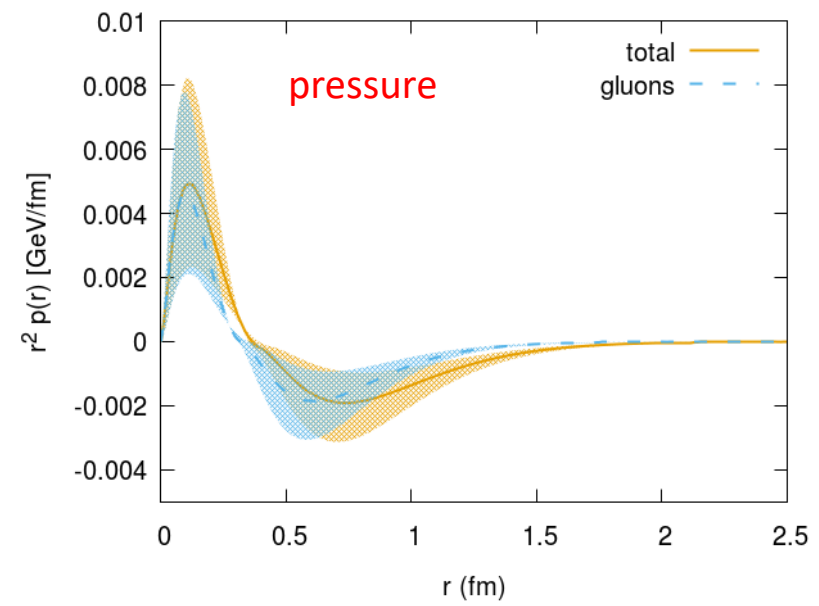
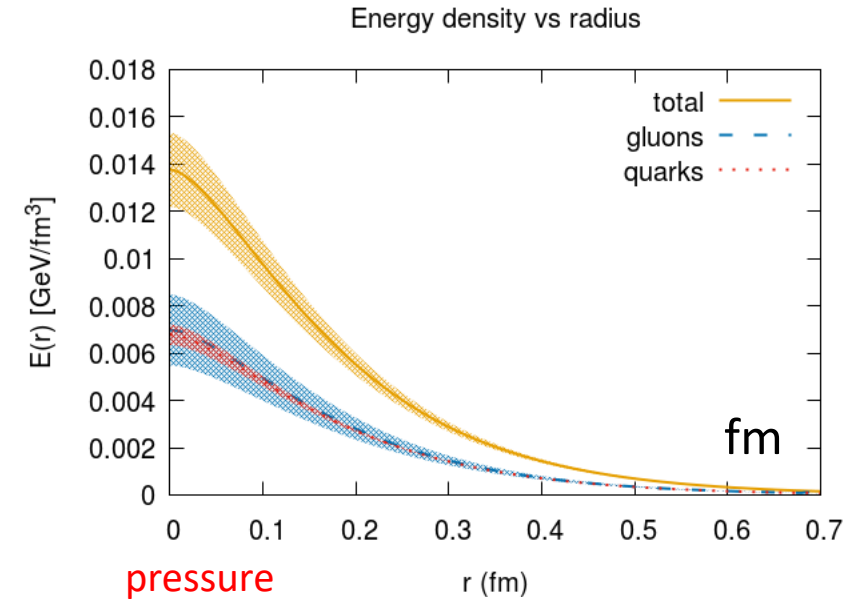
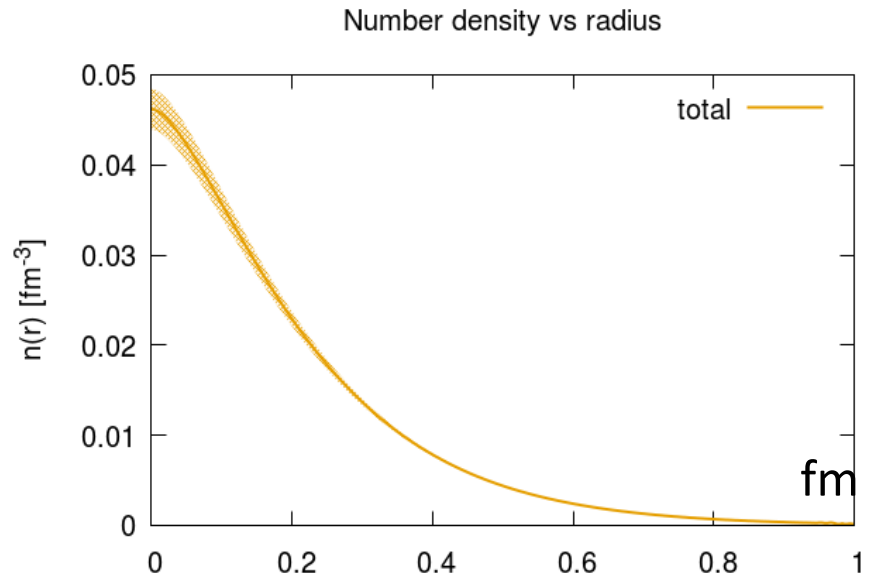
$$\epsilon_{q,g}(r) = \int \frac{d^2 \Delta_T}{(2\pi)^2} e^{i\Delta_T \cdot \mathbf{b}} A_2^{q,g}(t)$$

Energy density

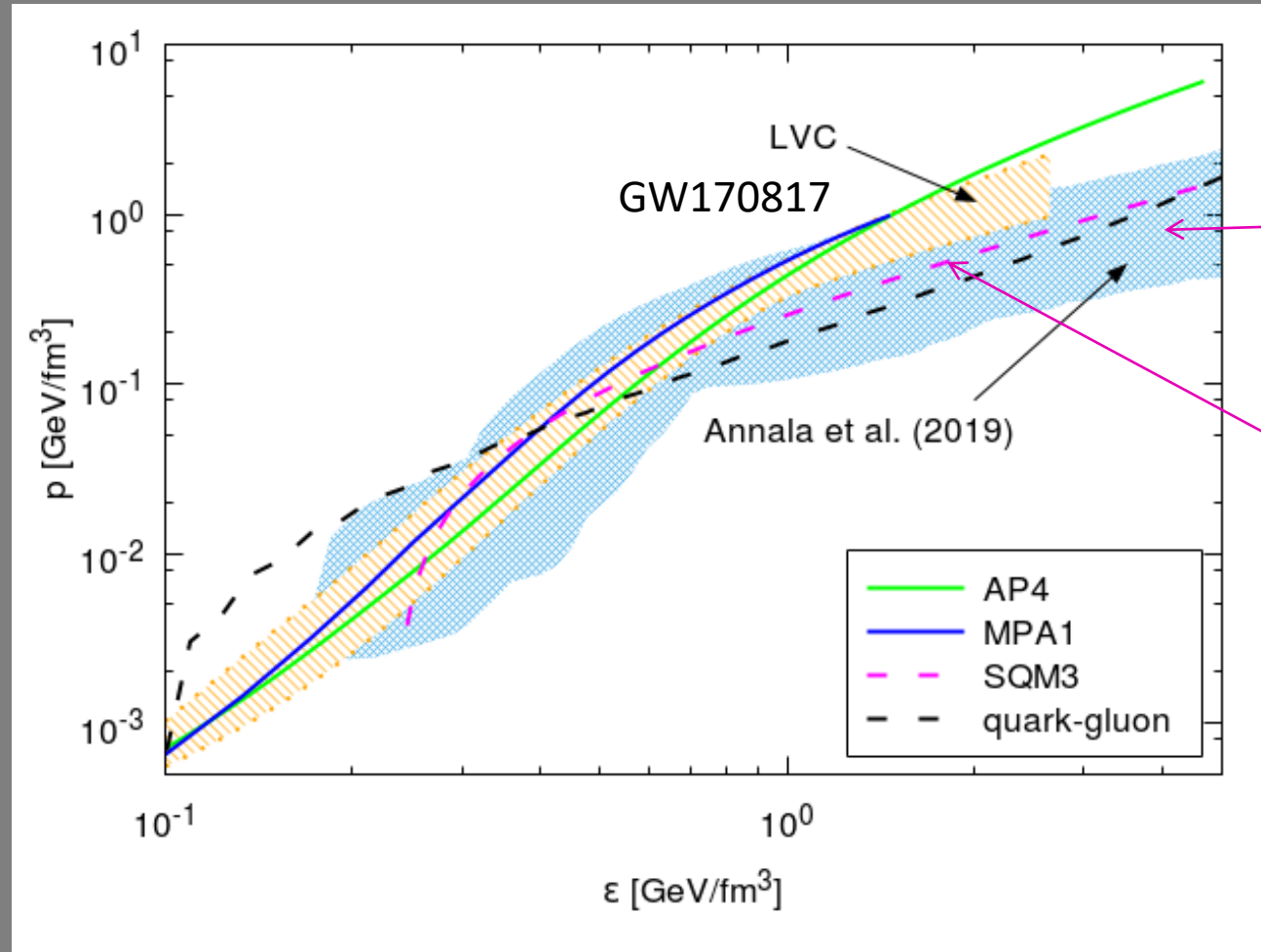
$$r = |\vec{\mathbf{b}}|$$

$$p_{q,g}(r) = \int \frac{d^2 \Delta_T}{(2\pi)^2} e^{i\Delta_T \cdot \mathbf{b}} 2t C_2^{q,g}(t)$$

Pressure



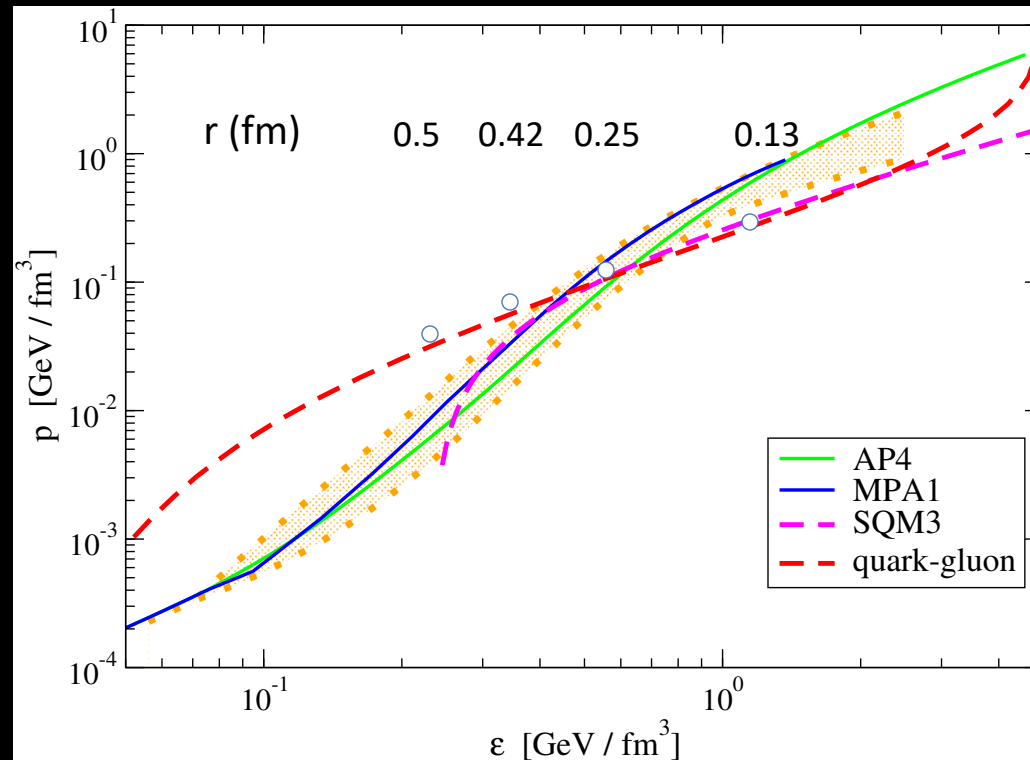
Detmold, Shahanan, Phys.Rev.Lett. 122 (2019)

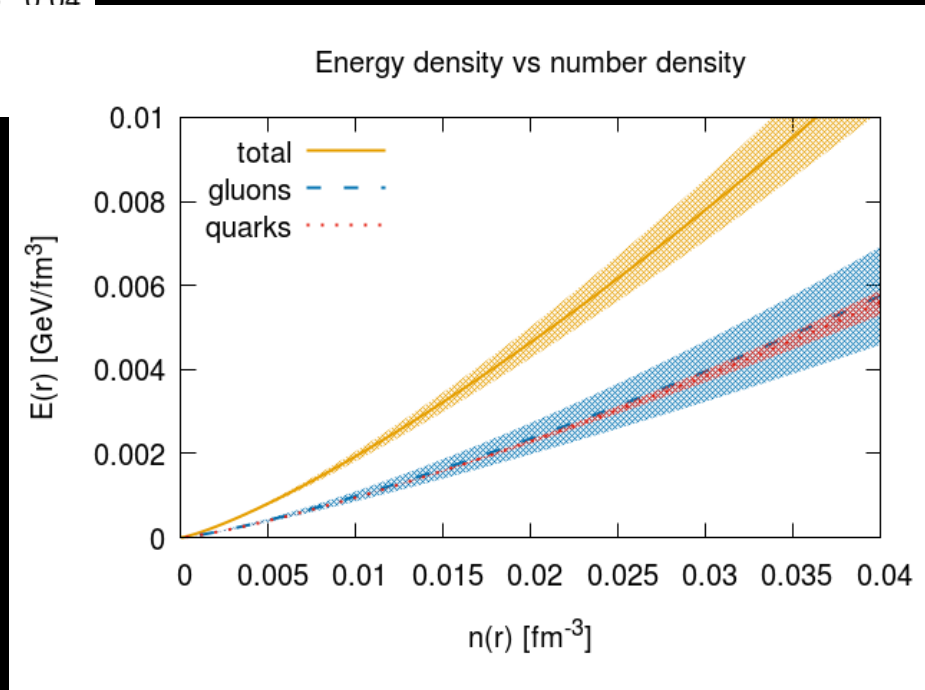
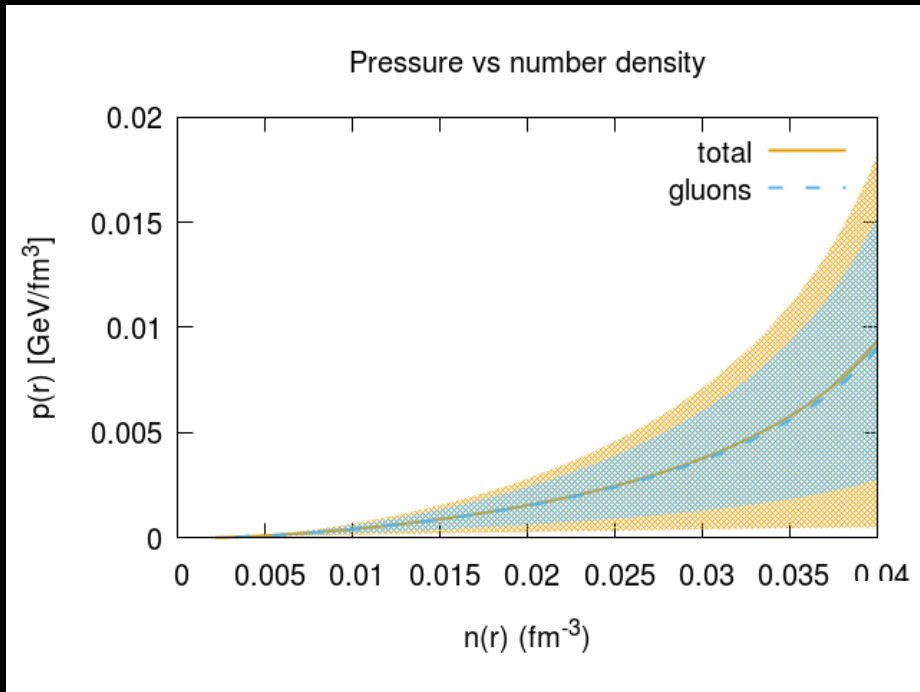


QCD EMT

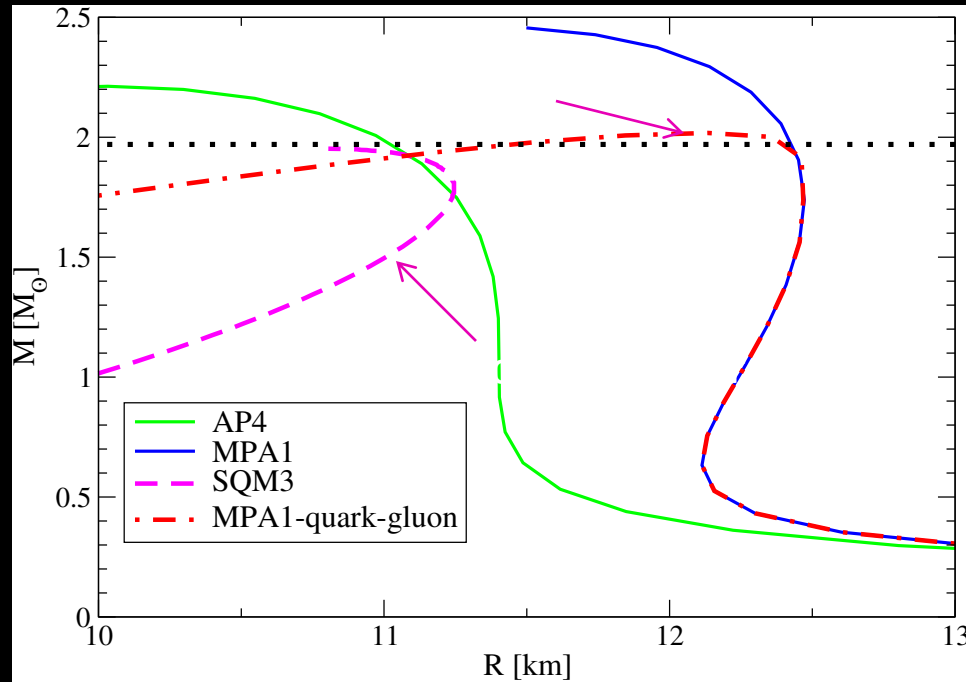
MIT bag model: strange quark matter

E (GeV/fm ³)	r (fm)
0.2	0.48
0.3	0.426
0.6	0.325
1	0.25
2	0.134
3	0.05





Rajan, Gorda, SL, Yagi, arXiv:1812.01479



J0348+0432 pulsar mass

“stitching” at transition pressure $0.15 \text{ GeV}/\text{fm}^3$

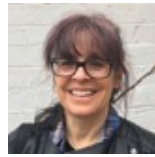
Jefferson Lab's measurement on the pressure inside the nucleon/hadronic matter needs to be corroborated by an independent set of measurements

Neutron stars mergers/multimessenger astronomy provide an independent constraint

WHAT'S NEXT...

Key question: how to extract accurate information on the mechanical properties of the nucleon from data

Summer Institute for Wigner Imaging and Femtography



Simonetta Liuti

Principle Investigator
University of Virginia



Matthias Burkardt

Co Principle Investigator
New Mexico State University



Pete Alonzi

Co Principle Investigator
University of Virginia



Dustin Keller

Co Principle Investigator
University of Virginia



Olivier Pfister

Co Principle Investigator
University of Virginia

Wigner Theory



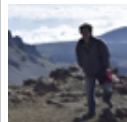
Librado Anglero

University of Virginia
Physics



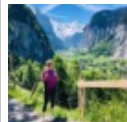
Fatma Aslan

New Mexico State University
PhD



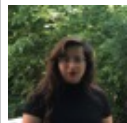
Kyle-Thomas Pressler

University of Virginia
Physics



Emma Yeats

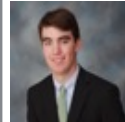
University of Virginia
Physics



Fernanda Yepez-Lopez

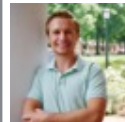
University of Virginia
Mathematics

Machine Learning



Jake Grigsby

Machine Learning Group Leader
University of Virginia
Computer Science and Mathematics



Evan Anders Magnusson

University of Virginia
Computer Engineering and
Computer Science



Christopher Thompson

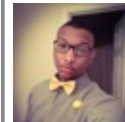
Virginia Union University
Physics and Engineering

Observables



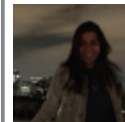
Brandon Kriesten

University of Virginia
Observables Group Leader



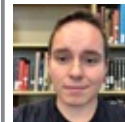
Krisean D Allen

Virginia Union University
Physics



Meg Graham

University of Virginia
Computer Science



Andrew Meyer

University of Virginia



William A Oliver

Virginia Commonwealth University



Yelena Prok

Virginia Commonwealth University
Assistant Professor

Data Management/ Communication



Yao(Grace) Tong

University of Virginia
Mathematics and Economics

Consultant



Carlos Gonzalez Arciniegas

University of Virginia



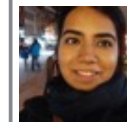
Timothy John Hobbs

Southern Methodist University
EIC Center at Jefferson Lab



Gabriel Niculescu

James Madison University



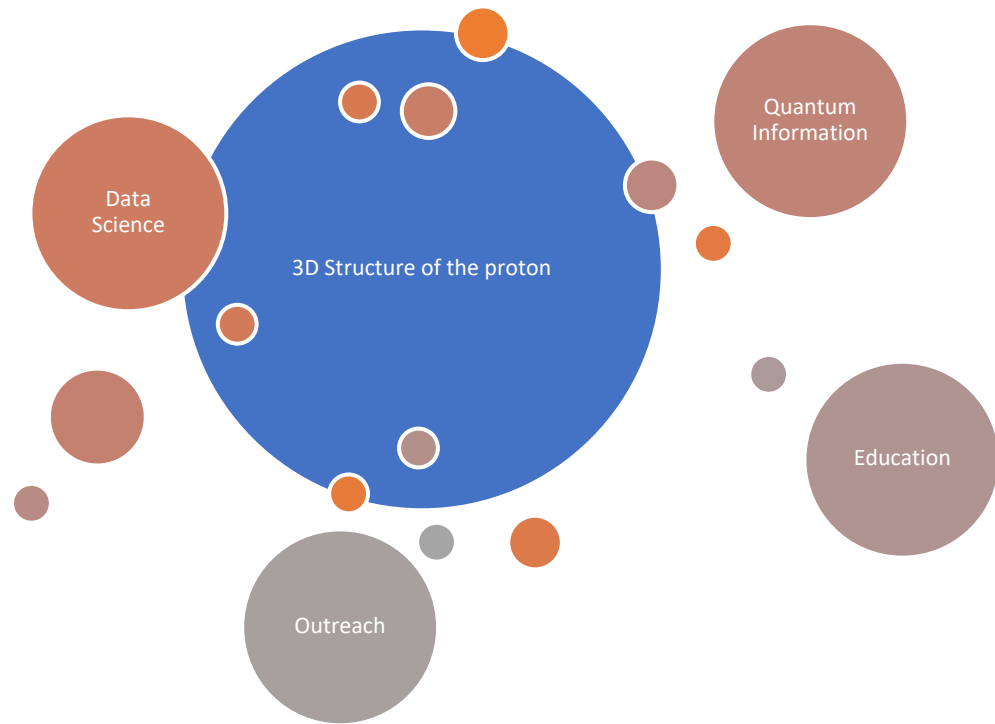
Abha Rajan

University of Virginia

Red: Undergraduate

Blue: Graduate

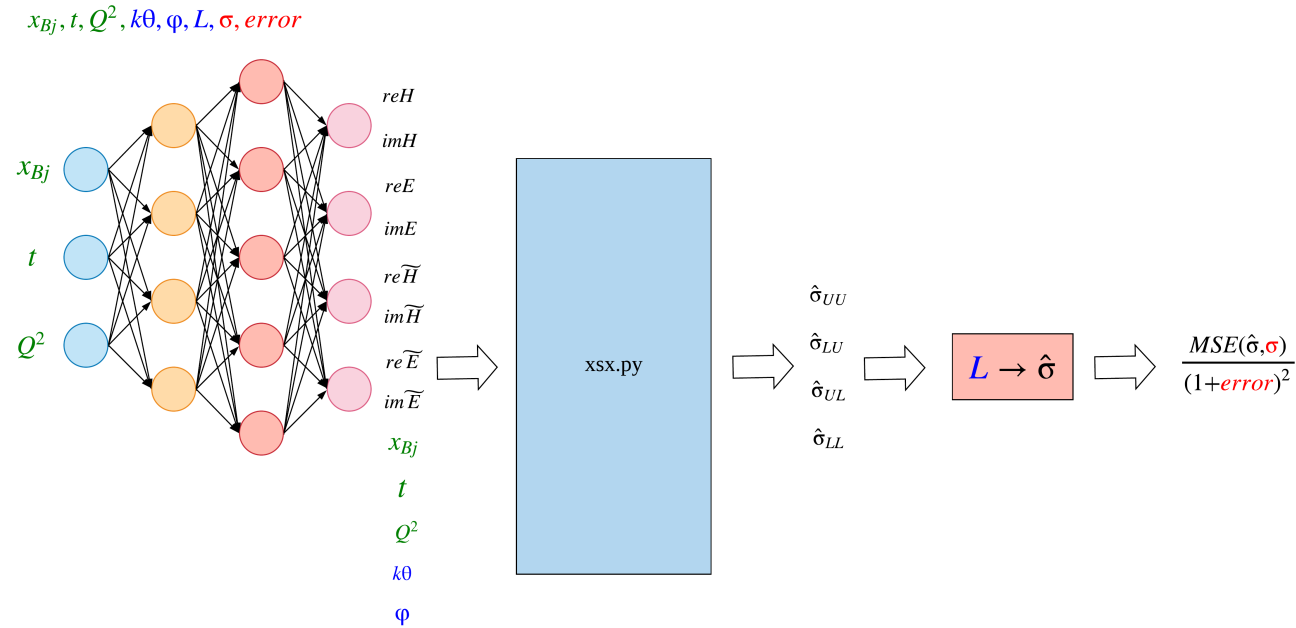
A truly interdisciplinary effort



Femtography Imaging with Neural Networks (FINN)

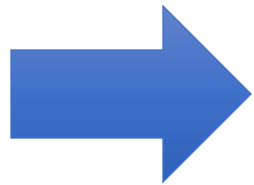
Strategy:

1. A fully connected neural network maps input kinematic data to a vector of eight form factors (see diagram).
2. Use a code developed by our Data Analysis Team to evaluate the **cross sections** and in terms of the CFFs.



Jake Grigsby

We translate the x-sec. code into **TensorFlow**

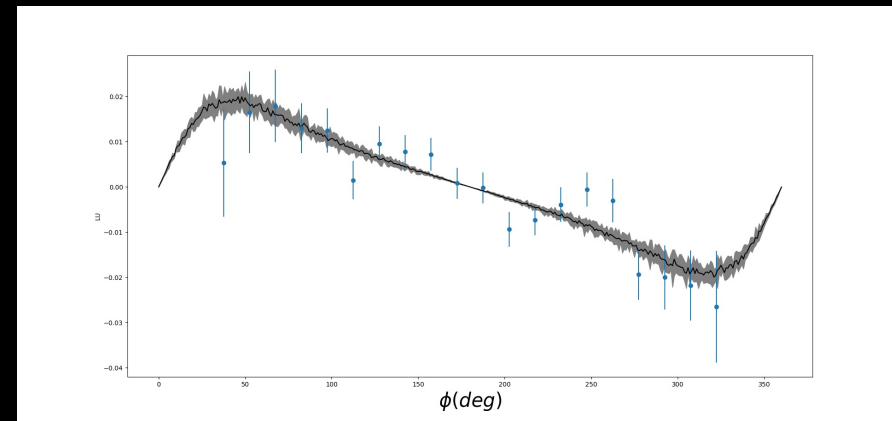
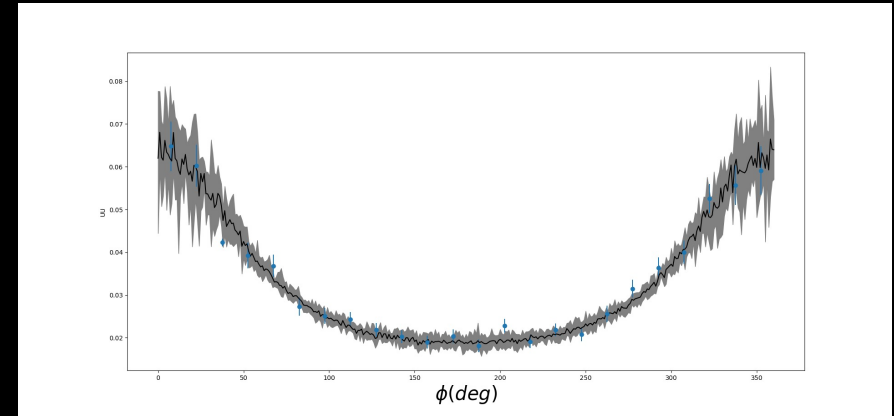
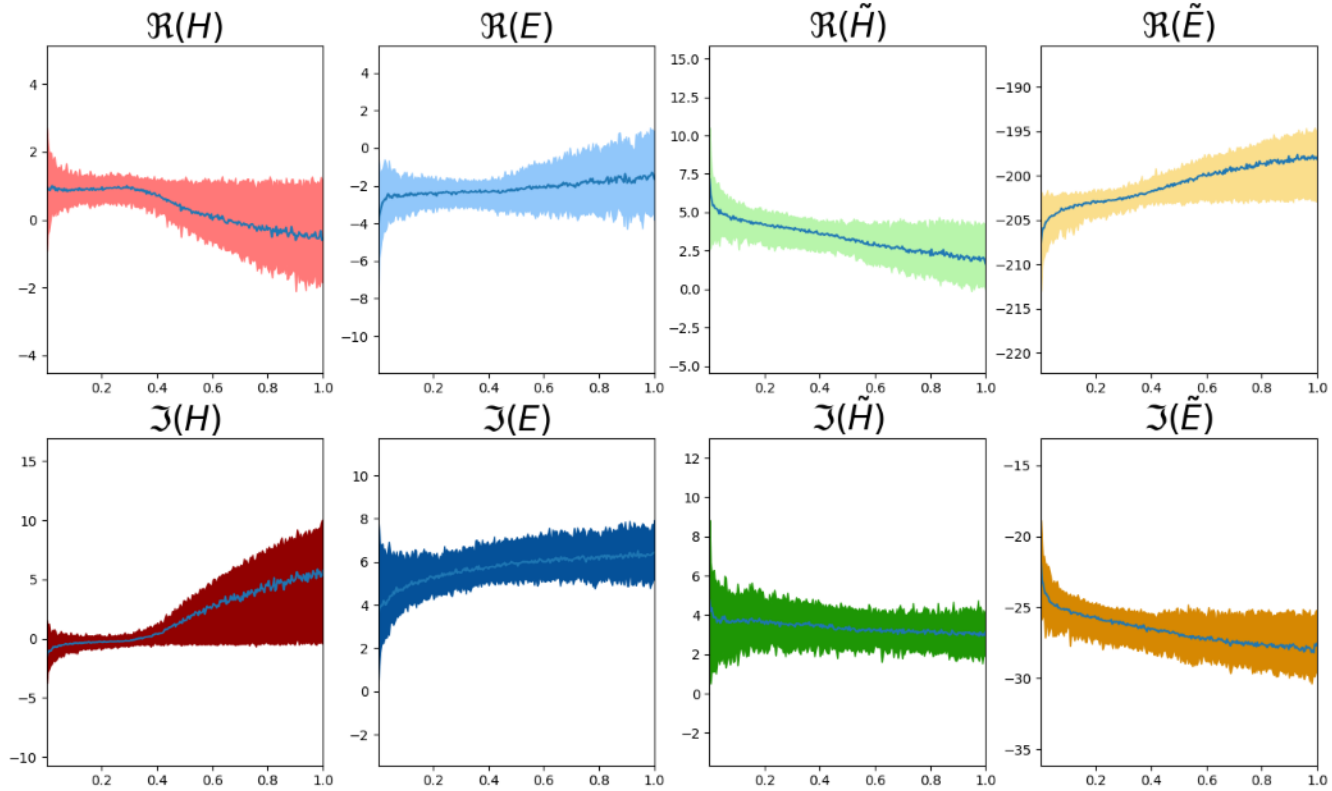


➔ Automatically differentiable

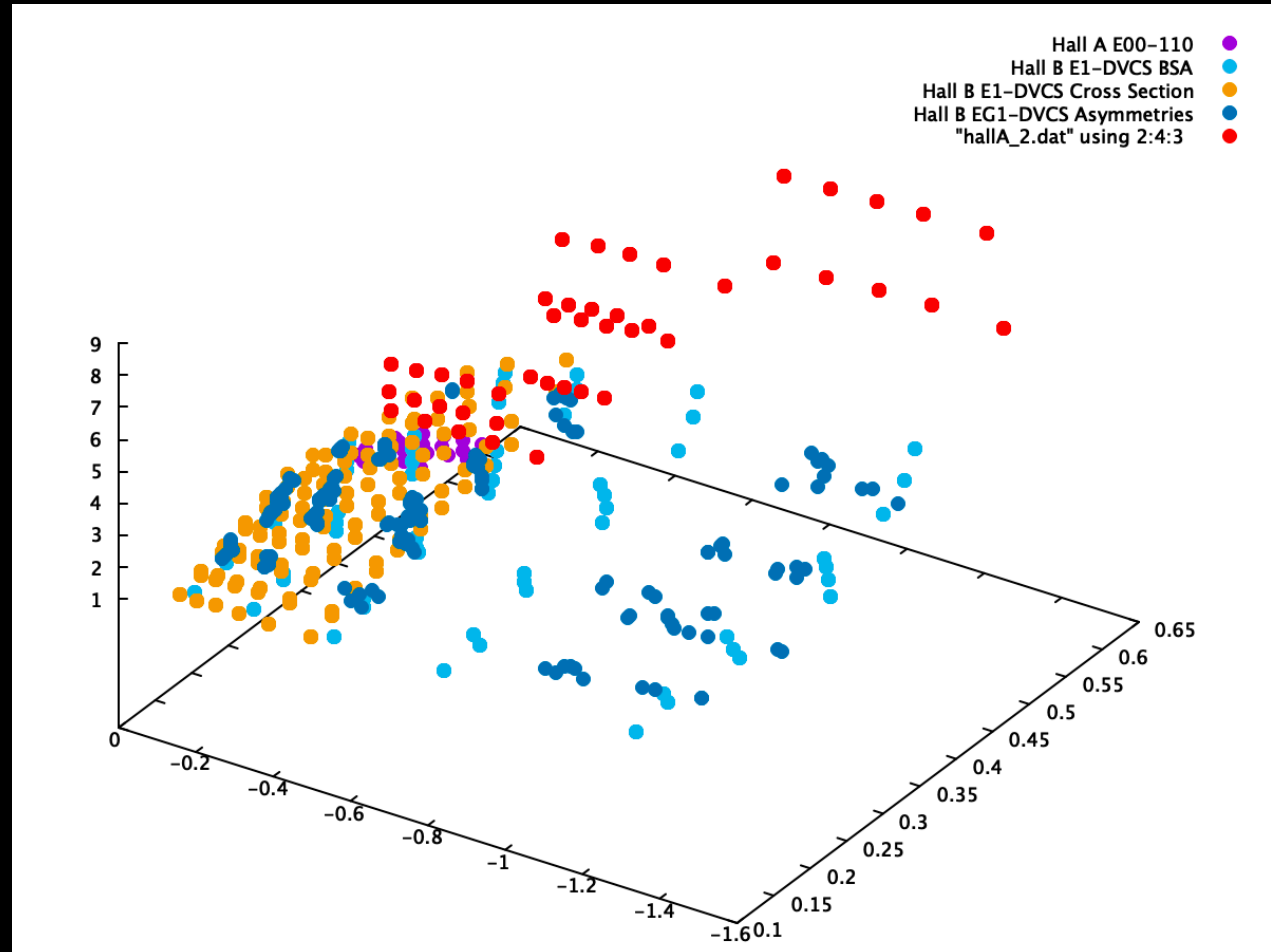
➔ At variance with other efforts we can train CFF extraction network with **backpropagation** and variants of **stochastic gradient descent**.

Compton Form factors

x_B Dependence



Jlab DVCS data



Introducing the complete formalism where all kinematical dependences and approximations are under control

arXiv:1903.05742

Extraction of Generalized Parton Distribution Observables from Deeply Virtual Electron Proton Scattering Experiments

Brandon Kriesten,^{*} Simonetta Liuti,[†] Liliet Calero Diaz,[‡] Dustin Keller,[§] and Andrew Meyer[¶]

Department of Physics, University of Virginia, Charlottesville, VA 22904, USA.

Gary R. Goldstein^{**}

Department of Physics and Astronomy, Tufts University, Medford, MA 02155 USA.

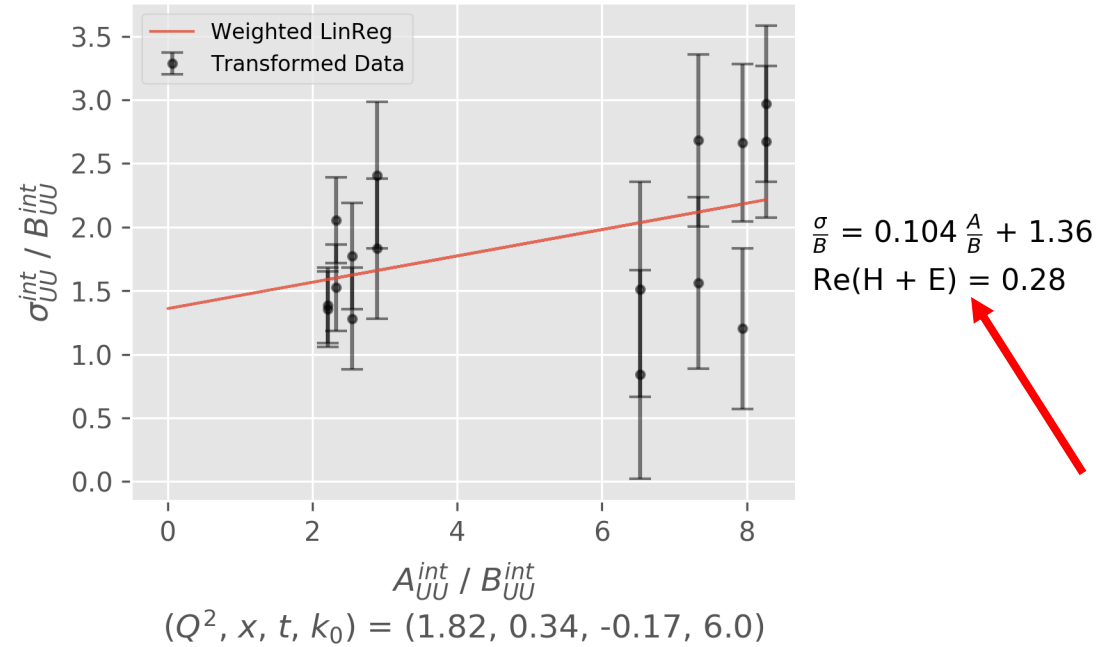
J. Osvaldo Gonzalez-Hernandez^{††}

INFN, Torino
(Dated: April 6, 2019)

We provide the general expression of the cross section for exclusive deeply virtual photon electroproduction from a spin 1/2 target using current parameterizations of the off-forward correlation function in a nucleon for different beam and target polarization configurations up to twist three accuracy. All contributions to the cross section including deeply virtual Compton scattering, the Bethe-Heitler process, and their interference, are described within a helicity amplitude based framework which is also relativistically covariant and readily applicable to both the laboratory frame and in a collider kinematic setting. Our formalism renders a clear physical interpretation of the various components of the cross section by making a connection with the known characteristic structure of the electron scattering coincidence reactions. In particular, we focus on the total angular momentum, J_z , and on the orbital angular momentum, L_z . On one side, we uncover an avenue to a precise extraction of J_z , given by the combination of generalized parton distributions, $H + E$, through a generalization of the Rosenbluth separation method used in elastic electron proton scattering. On the other, we single out for the first time, the twist three angular modulations of the cross section that are sensitive to L_z . The proposed generalized Rosenbluth technique adds constraints and can

Brandon Kriesten, talk Tuesday

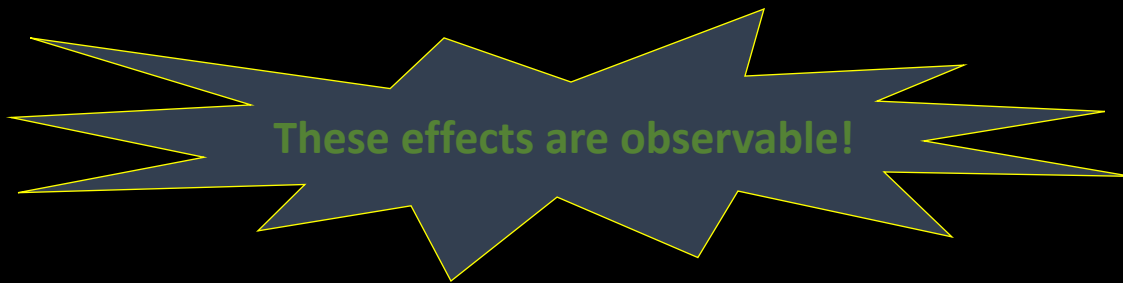
Interference Rosenbluth Separation



$$\frac{d^3 \sigma_{unpol}^{\perp}}{dx_{Bj} dQ^2 d|t| d\phi d\phi_S} = \frac{\Gamma}{Q^2(-t)} \left[A_I \overbrace{(F_1 \Re \mathcal{H} + \tau F_2 \Re \mathcal{E})}^{G_E^2 + \tau G_M^2} + B_I \overbrace{G_M \Re(\mathcal{H} + \mathcal{E})}^{G_M^2} + C_I \overbrace{G_M \Re \tilde{\mathcal{H}}}^{G_M G_A} \right]$$

Conclusions and Outlook

- The EoS of dense matter in QCD can be obtained from first principles, using **ab initio calculations for both quark and gluon d.o.f.**
- **Gluons** are found to dominate the EoS providing a trend in the high density regime which is consistent with the constraint from LIGO.



- We can connect the **pressure and energy density** in neutron stars with collider observables: the **GPDs**.
- The proposed line of research opens up a new framework for understanding the properties of **hybrid stars**. In the future we hope to set more stringent constraints on the nature of the **hadron to quark matter transition** at zero temperature.

...To observe, evaluate and interpret

Wigner distributions at the subatomic level

**requires stepping up data analyses from the standard methods →
developing new numerical/analytic/quantum computing methods**



Center for Nuclear Femtography Project

